Classical strongly coupled quark-gluon plasma. VI. Shear viscosity and self-diffusion

Sungtae Cho and Ismail Zahed

Department of Physics and Astronomy, State University of New York, Stony Brook, New York 11794-3800, USA

(Received 10 December 2009; revised manuscript received 28 August 2010; published 23 November 2010)

We construct the Liouville operator for the SU(2) classical colored Coulomb plasma for arbitrary values of the Coulomb coupling $\Gamma = V/K$, the ratio of the mean Coulomb to kinetic energy. We show that its resolvent in the classical colored phase space obeys a hierarchy of equations. We use a free-streaming approximation to close the hierarchy and derive an integral equation for the time-dependent structure factor. Its reduction by projection yields hydrodynamical equations in the long-wavelength limit. We discuss the character of the hydrodynamical modes at strong coupling. The shear viscosity is shown to exhibit a minimum at $\Gamma \approx 8$ near the liquid point. This minimum follows from the crossover between the single-particle collisional regime which drops as $1/\Gamma^{5/2}$ and the hydrodynamical collisional regime which rises as $\Gamma^{1/2}$. The self-diffusion constant drops as $1/\Gamma^{3/2}$ irrespective of the regime. We compare our results to molecular-dynamics simulations of the SU(2) colored Coulomb plasma. We also discuss the relevance of our results for the quantum and strongly coupled quark-gluon plasma (sQGP).

DOI: 10.1103/PhysRevC.82.054907 PACS number(s): 12.38.Mh, 25.75.Nq, 51.20.+d, 52.27.Gr

I. INTRODUCTION

High-temperature QCD is expected to asymptote a weakly coupled Coulomb plasma albeit with still strong infrared divergences. The latter causes its magnetic sector to be nonperturbative at all temperatures. At intermediate temperatures of relevance to heavy-ion collider experiments, the electric sector is believed to be strongly coupled.

Recently, Shuryak and Zahed [1] have suggested that certain aspects of the quak-gluon plasma in range of temperatures $(1-3)\,T_c$ can be understood by a stronger Coulomb interaction causing persistent correlations in singlet and colored channels. As a result the quark and gluon plasma is more a liquid than a gas at intermediate temperatures. A liquid plasma should exhibit shorter mean free paths and stronger color dissipation, both of which are supported by the current experiments at RHIC [2].

To help understand transport and dissipation in the strongly coupled quark-gluon plasma, a classical model of the colored plasma was suggested in [3]. The model consists of massive quarks and gluons interacting via classical colored Coulomb interactions. The color is assumed classical with all equations of motion following from Poisson brackets. For the SU(2) version both molecular-dynamics simulations [3] and bulk thermodynamics [4,5] were recently presented, including simulations of the energy loss of heavy quarks [6].

This classical model description is based on the quasiparticle behavior of quarks and gluons at temperature near T_c. Their masses in that region are in the order of 3T [7]. Therefore, these particles can be treated classically and nonrelativistically, which makes it possible to ignore color magnetic effects in the following argument.

In this paper we extend our recent equilibrium analysis of the static properties of the classical quark-gluon plasma (cQGP), to transport. In Sec. II we discuss the classical equations of motion in the SU(2) colored phase space and derive the pertinent Liouville operator. In Sec. III we show that the resolvent of the Liouville operator obeys a hierarchy of equations in the SU(2) phase space. In Sec. IV we derive an integral equation for the time-dependent structure factor by introducing a nonlocal self-energy kernel in phase space. In Sec. V we close the Liouville hierarchy through a free-streaming approximation on the four-point resolvent and derive the self-energy kernel in closed form. In Sec. VI we project the self-energy kernel and the nonstatic structure factor onto the colorless hydrodynamical phase space. In Sec. VII we show that the sound and plasmon mode are the leading hydrodynamical modes in the SU(2) colored Coulomb plasma. In Sec. VIII we analyze the shear viscosity for the transverse sound mode for arbitrary values of Γ. We show that a minimum forms at $\Gamma \approx 5$ at the crossover between the hydrodynamical and single-particle regimes. In Sec. IX we analyze self-diffusion in phase space, and derive an explicit expression for the diffusion constant at strong coupling. Our conclusions and prospects are in Sec. X. In Appendix A we briefly summarize our variables in the SU(2) phase space. In Appendix B we detail the projection method for the self-energy kernel used in the text. In Appendix C we show that the collisional color contribution to the Liouville operator drops in the self-energy kernel. In Appendix D some useful aspects of the hydrodynamical projection method are outlined.

II. COLORED LIOUVILLE OPERATOR

The canonical approach to the colored Coulomb plasma was discussed in [3]. In brief, the Hamiltonian for a single species of constituent quarks or gluons in the SU(2) representation is defined as

$$H = \sum_i^N \frac{\boldsymbol{p}_i^2}{2m_i} + \sum_{i>j=1}^N \frac{\boldsymbol{Q}_i \cdot \boldsymbol{Q}_j}{|\boldsymbol{r}_i - \boldsymbol{r}_j|}. \tag{2.1}$$

The charge $g^2/4\pi$ has been omitted for simplicity of the notation flow and will be reinserted in the pertinent physical quantities by inspection.

The equations of motion in phase space follows from the classical Poisson brackets. In particular

$$\frac{d\boldsymbol{r}_i}{dt} = -\{H, \boldsymbol{r}_i\} = \frac{\partial H}{\partial \boldsymbol{p}_j}\frac{\partial \boldsymbol{r}_i}{\partial \boldsymbol{r}_j} = \frac{\boldsymbol{p}_i}{m}. \tag{2.2}$$

The Newtonian equation of motion is just the colored electric Lorentz force

$$\frac{d\boldsymbol{p}_i}{dt} = -\{H, \boldsymbol{p}_i\} = -\frac{\partial H}{\partial \boldsymbol{r}_j}\frac{\partial \boldsymbol{p}_i}{\partial \boldsymbol{p}_j} = Q_i^a \boldsymbol{E}_i^a = \boldsymbol{F}_i \tag{2.3}$$

with the colored electric field and potentials defined as ($a = 1, 2, 3$)

$$\boldsymbol{E}_i^a = -\nabla_i \Phi_i^a = -\nabla_i \sum_{j\neq i} \frac{Q_j^a}{|\boldsymbol{r}_i - \boldsymbol{r}_j|}. \tag{2.4}$$

Our strongly coupled colored plasma is mostly electric following the original assumptions in [3,8]. The equation of motion of the color charges is

$$\begin{aligned}\frac{dQ_i^a}{dt} &= -\left\{H, Q_i^a\right\} = -\sum_{j,b}\frac{\partial H}{\partial Q_i^b}\frac{\partial Q_i^a}{\partial Q_j^c}\left\{Q_j^b, Q_j^c\right\} \\ &= \sum_{j\neq i}\frac{Q_i T^a Q_j}{|\boldsymbol{r}_i - \boldsymbol{r}_j|}\end{aligned} \tag{2.5}$$

for arbitrary color representation. For SU(2) the classical color charge (2.5) precesses around the net colored potential Φ determined by the other particles as defined in (2.4),

$$\frac{d\boldsymbol{Q}_i}{dt} = (\boldsymbol{\Phi}_i \times \boldsymbol{Q}_i). \tag{2.6}$$

This equation was initially derived by Wong [9]. Some aspects of the SU(2) phase space are briefly recalled in Appendix A.

The set (2.2), (2.3), and (2.5) define the canonical evolution in phase space. The time-dependent phase distribution is formally given by

$$\begin{aligned}f(t, \boldsymbol{r}\,\boldsymbol{p}\,\boldsymbol{Q}) &= \sum_{i=1}^{N}\delta[\boldsymbol{r} - \boldsymbol{r}_i(t)]\delta[\boldsymbol{p} - \boldsymbol{p}_i(t)]\delta[\boldsymbol{Q} - \boldsymbol{Q}_i(t)] \\ &\equiv \sum_i \delta[\boldsymbol{q} - \boldsymbol{q}_i(t)].\end{aligned} \tag{2.7}$$

For simplicity $\boldsymbol{q}$ is generic for $\boldsymbol{r}$, $\boldsymbol{p}$, $\boldsymbol{Q}$. Using the chain rule, the time-evolution operator on (2.7) obeys

$$\frac{d}{dt} = \frac{\partial}{\partial t} + \frac{d\boldsymbol{r}_i}{dt}\frac{\partial}{\partial \boldsymbol{r}_i} + \frac{d\boldsymbol{p}_i}{dt}\frac{\partial}{\partial \boldsymbol{p}_i} + \frac{d\boldsymbol{Q}_i}{dt}\frac{\partial}{\partial \boldsymbol{Q}_i} \equiv \partial_t + i\mathcal{L}. \tag{2.8}$$

The last relation defines the Liouville operator

$$\begin{aligned}\mathcal{L} &= \mathcal{L}_0 + \mathcal{L}_I + \mathcal{L}_Q \\ &= -i\boldsymbol{v}_i \cdot \nabla_{r_i} - i\,\boldsymbol{F}_i \cdot \nabla_{p_i} - i\boldsymbol{\Phi}_i \cdot (\boldsymbol{Q}_i \times \nabla_{Q_i}).\end{aligned} \tag{2.9}$$

The last contribution in (2.9) is genuinely a three-body force because of the cross product (orbital color operator). It requires three distinct colors to not vanish. This observation will be important in simplifying the color dynamics below. Also (2.9) is Hermitian.

Since (2.7) depends implicitly on time, we can write formally

$$\frac{d}{dt} f(t, \boldsymbol{r}\,\boldsymbol{p}\,\boldsymbol{Q}) = i\mathcal{L} f(t, \boldsymbol{r}\,\boldsymbol{p}\,\boldsymbol{Q}) \tag{2.10}$$

with a solution $f(t) = e^{i\mathcal{L}t} f(0)$. The formal relation (2.10) should be considered with care since the action of the Liouville operator on the one-body phase-space distribution (2.7) generates also a two-body phase-space distribution. Indeed, while $\mathcal{L}_0$ is local in phase space

$$\begin{aligned}\mathcal{L}_0 \sum_i \delta(\boldsymbol{q} - \boldsymbol{q}_i) &= -i\boldsymbol{v} \cdot \nabla_r \sum_i \delta(\boldsymbol{q} - \boldsymbol{q}_i) \\ &= L_0(\boldsymbol{q}) \sum_i \delta(\boldsymbol{q} - \boldsymbol{q}_i)\end{aligned} \tag{2.11}$$

the two other contributions are not. Specifically

$$\begin{aligned}&\mathcal{L}_I \sum_m \delta(\boldsymbol{q} - \boldsymbol{q}_m) \\ &= i\sum_{i\neq j} \nabla_{r_i}\frac{\boldsymbol{Q}_i \cdot \boldsymbol{Q}_j}{|\boldsymbol{r}_i - \boldsymbol{r}_j|} \cdot \nabla_{p_i} \sum_m \delta(\boldsymbol{q} - \boldsymbol{q}_m) \\ &= i\int d\boldsymbol{q}' \sum_{i\neq j,mn} \nabla_{r_i}\frac{\boldsymbol{Q}_i \cdot \boldsymbol{Q}_j}{|\boldsymbol{r}_i - \boldsymbol{r}_j|} \cdot \nabla_{p_i}\, \delta(\boldsymbol{q} - \boldsymbol{q}_m)\delta(\boldsymbol{q}' - \boldsymbol{q}_n) \\ &= -\int d\boldsymbol{q}' L_I(\boldsymbol{q}, \boldsymbol{q}') \sum_{mn} \delta(\boldsymbol{q} - \boldsymbol{q}_m)\delta(\boldsymbol{q}' - \boldsymbol{q}_n)\end{aligned} \tag{2.12}$$

with

$$L_I(\boldsymbol{q}, \boldsymbol{q}') = i\nabla_r \frac{\boldsymbol{Q} \cdot \boldsymbol{Q}'}{|\boldsymbol{r} - \boldsymbol{r}'|} \cdot (\nabla_p - \nabla_{p'}). \tag{2.13}$$

Similarly

$$\begin{aligned}&\mathcal{L}_Q \sum_m \delta(\boldsymbol{q} - \boldsymbol{q}_m) \\ &= -i\sum_{j\neq i,m} \frac{\boldsymbol{Q}_i \times \boldsymbol{Q}_j}{|\boldsymbol{r}_i - \boldsymbol{r}_j|} \cdot \nabla_{Q_i}\, \delta(\boldsymbol{q} - \boldsymbol{q}_m) \\ &= -i\int d\boldsymbol{q}' \sum_{j\neq i,mn} \frac{\boldsymbol{Q}_i \times \boldsymbol{Q}_j}{|\boldsymbol{r}_i - \boldsymbol{r}_j|} \cdot \nabla_{Q_i}\delta(\boldsymbol{q} - \boldsymbol{q}_m)\delta(\boldsymbol{q}' - \boldsymbol{q}_n) \\ &= -\int d\boldsymbol{q}' L_Q(\boldsymbol{q}, \boldsymbol{q}') \sum_{mn} \delta(\boldsymbol{q} - \boldsymbol{q}_m)\delta(\boldsymbol{q}' - \boldsymbol{q}_n)\end{aligned} \tag{2.14}$$

with

$$L_Q(\boldsymbol{q}, \boldsymbol{q}') = -i\frac{\boldsymbol{Q} \times \boldsymbol{Q}'}{|\boldsymbol{r} - \boldsymbol{r}'|} \cdot (\nabla_Q - \nabla_{Q'}). \tag{2.15}$$

Clearly (2.14) drops from two-body and symmetric phase-space distributions. It does not for three-body and higher.

III. LIOUVILLE HIERARCHY

An important correlation function in the analysis of the colored Coulomb plasma is the time-dependent structure factor or two-body correlation in the color phase space

$$\mathbf{S}(t - t', \boldsymbol{r} - \boldsymbol{r}', \boldsymbol{p}\boldsymbol{p}', \boldsymbol{Q} \cdot \boldsymbol{Q}') = \langle \delta f(t, \boldsymbol{r}\,\boldsymbol{p}\,\boldsymbol{Q})\, \delta f(t', \boldsymbol{r}'\boldsymbol{p}'\,\boldsymbol{Q}')\rangle \tag{3.1}$$

with $\delta f = f - \langle f \rangle$ the shifted one-body phase-space distribution. The averaging in (3.1) is carried over the initial conditions with a fixed number of particles N and average energy or temperature $\beta = 1/T$. Thus $\langle f \rangle = n f_0(p)$ which is the Maxwellian distribution for constituent quarks or gluons. In equilibrium, the averaging in (3.1) is time and space translational invariant as well as color-rotational invariant.

Using the ket notation with $\mathbf{1} \equiv \boldsymbol{q} \equiv \boldsymbol{r}\,\boldsymbol{p}\,\boldsymbol{Q}$

$$|\delta f(t,\mathbf{1})\rangle = \Big|\sum_m \delta[\boldsymbol{q} - \boldsymbol{q}_m(t)] - \Big\langle \sum_m \delta[\boldsymbol{q} - \boldsymbol{q}_m(t)]\Big\rangle\Big\rangle \equiv |\delta f(t,\mathbf{1}) - \langle f(t,\mathbf{1})\rangle\rangle \tag{3.2}$$

with also $\mathbf{2} = \boldsymbol{q}'$, $\mathbf{3} = \boldsymbol{q}''$, $\mathbf{4} = \boldsymbol{q}'''$, and so on and the formal Liouville solution $\delta f(t,\mathbf{1}) = e^{i\mathcal{L}t}\delta f(\mathbf{1})$, we can write (3.1) as

$$\mathbf{S}(t-t',\boldsymbol{q},\boldsymbol{q}') = \langle \delta f(t,\mathbf{1})|\delta f(t',\mathbf{2})\rangle = \langle \delta f(\mathbf{1})|e^{i\mathcal{L}(t'-t)}|\delta f(\mathbf{2})\rangle. \tag{3.3}$$

The bra-ket notation is short for the initial or equilibrium average. Its Laplace or causal transform reads

$$\mathbf{S}(z,\boldsymbol{q},\boldsymbol{q}') = -i\int_{-\infty}^{+\infty} dt\,\theta(t-t')\,e^{izt}\,\mathbf{S}(t-t',\boldsymbol{q},\boldsymbol{q}') = \langle \delta f(\mathbf{1})|\frac{1}{z+\mathcal{L}}|\delta f(\mathbf{2})\rangle \tag{3.4}$$

with $z = \omega + i0$. Clearly

$$z\mathbf{S}(z,\boldsymbol{q},\boldsymbol{q}') + \langle \delta f(\mathbf{1})|\mathcal{L}\frac{1}{z+\mathcal{L}}|\delta f(\mathbf{2})\rangle = \langle \delta f(\mathbf{1})|\delta f(\mathbf{2})\rangle. \tag{3.5}$$

Since $\mathcal{L}^\dagger = \mathcal{L}$ is Hermitian and using (2.11), (2.12), and (2.14), it follows that

$$\langle \delta f(\mathbf{1})|\mathcal{L} = \langle \delta f(\mathbf{1})|L_0(\boldsymbol{q}) - \int d\boldsymbol{q}''\,L_{I+Q}(\boldsymbol{q},\boldsymbol{q}'')\,\langle \delta f(\mathbf{1})\delta f(\mathbf{3})|. \tag{3.6}$$

Thus

$$[z - L_0(\boldsymbol{q})]\mathbf{S}(z,\boldsymbol{q},\boldsymbol{q}') - \int d\boldsymbol{q}''L_{I+Q}(\boldsymbol{q}',\boldsymbol{q}'')\mathbf{S}(z,\boldsymbol{q}\boldsymbol{q}'',\boldsymbol{q}') = \mathbf{S}_0(\boldsymbol{q},\boldsymbol{q}'), \tag{3.7}$$

where we have defined the three-body phase-space resolvent

$$\mathbf{S}(z,\boldsymbol{q}\boldsymbol{q}'',\boldsymbol{q}') = \langle \delta f(\mathbf{1})\delta f(\mathbf{3})|\frac{1}{z+\mathcal{L}}|\delta f(\mathbf{2})\rangle. \tag{3.8}$$

$\mathbf{S}_0(\boldsymbol{q},\boldsymbol{q}')$ is the static colored structure factor discussed by us in [10]. Since $L_{I+Q}(\boldsymbol{q}',\boldsymbol{q})$ is odd under the switch $\boldsymbol{q} \leftrightarrow \boldsymbol{q}'$, and since $\mathbf{S}(z,\boldsymbol{q}\boldsymbol{q}'',\boldsymbol{q}') = \mathbf{S}(-z,\boldsymbol{q},\boldsymbol{q}'\boldsymbol{q}'')$ owing to the $t \leftrightarrow t'$ in (3.4), then

$$[z + L_0(\boldsymbol{q}')]\mathbf{S}(z,\boldsymbol{q},\boldsymbol{q}') - \int d\boldsymbol{q}''L_{I+Q}(\boldsymbol{q}',\boldsymbol{q}'')\mathbf{S}(z,\boldsymbol{q},\boldsymbol{q}'\boldsymbol{q}'') = \mathbf{S}_0(\boldsymbol{q},\boldsymbol{q}'). \tag{3.9}$$

Equation (3.7) or equivalently (3.9) defines the Liouville hierarchy, whereby the two-body phase-space distribution ties to the three-body phase-space distribution and so on. Indeed, (3.9), for instance, implies

$$[z + L_0(\boldsymbol{q}'')]\mathbf{S}(z,\boldsymbol{q}\boldsymbol{q}',\boldsymbol{q}'') - \int d\boldsymbol{q}'''L_{I+Q}(\boldsymbol{q}'',\boldsymbol{q}''')\mathbf{S}(z,\boldsymbol{q}\boldsymbol{q}',\boldsymbol{q}''\boldsymbol{q}''') = \mathbf{S}_0(\boldsymbol{q}\boldsymbol{q}',\boldsymbol{q}'') \tag{3.10}$$

with the four-point resolvent function

$$\mathbf{S}(z,\boldsymbol{q}\boldsymbol{q}',\boldsymbol{q}''\boldsymbol{q}''') = \langle \delta f(\mathbf{1})\delta f(\mathbf{2})|\frac{1}{z+\mathcal{L}}|\delta f(\mathbf{3})\delta f(\mathbf{4})\rangle. \tag{3.11}$$

These are the microscopic kinetic equations for the color phase-space distributions. They are only useful when closed, that is by a truncation as we discuss below. These formal equations were initially discussed in [11–14] in the context of the one-component Coulomb-Abelian-Coulomb plasma. We have now generalized them to the multicomponent and non-Abelian colored Coulomb plasma.

IV. SELF-ENERGY KERNEL

In (3.7) the nonlocal part of the Liouville operator plays the role of a nonlocal self-energy kernel Σ on the two-body resolvent. Indeed, we can rewrite (3.7) as

$$[z - L_0(\boldsymbol{q})]\mathbf{S}(z,\boldsymbol{q},\boldsymbol{q}') - \int d\boldsymbol{q}''\Sigma(z,\boldsymbol{q},\boldsymbol{q}'')\mathbf{S}(z,\boldsymbol{q}'',\boldsymbol{q}') = \mathbf{S}_0(\boldsymbol{q},\boldsymbol{q}') \tag{4.1}$$

with the nonlocal self-energy kernel defined formally as

$$\int d\boldsymbol{q}''\Sigma(z,\boldsymbol{q},\boldsymbol{q}'')\,\mathbf{S}(z,\boldsymbol{q}'',\boldsymbol{q}') = \int d\boldsymbol{q}''L_{I+Q}(\boldsymbol{q},\boldsymbol{q}'')\,\mathbf{S}(z,\boldsymbol{q}\boldsymbol{q}'',\boldsymbol{q}') \tag{4.2}$$

The self-energy kernel Σ can be regarded as the sum of a static or z-independent contribution Σ_S and a nonstatic or collisional contribution Σ_C,

$$\Sigma(z,\boldsymbol{q},\boldsymbol{q}'') = \Sigma_S(\boldsymbol{q},\boldsymbol{q}'') + \Sigma_C(z,\boldsymbol{q},\boldsymbol{q}''). \tag{4.3}$$

The stationary part Σ_S satisfies

$$\int d\boldsymbol{q}''\Sigma_S(\boldsymbol{q},\boldsymbol{q}'')\,\mathbf{S}_0(\boldsymbol{q}'',\boldsymbol{q}') = \int d\boldsymbol{q}''L_{I+Q}(\boldsymbol{q},\boldsymbol{q}'')\,\mathbf{S}_0(\boldsymbol{q},\boldsymbol{q}',\boldsymbol{q}''), \tag{4.4}$$

which identifies it with the sum of the two- and three-body part of the Liouville operator L_{I+Q}.

The collisional part Σ_C is more involved. To unwind it, we operate with $[z + L_0(\boldsymbol{q}')]$ on both sides of (4.2), and then reduce the left-hand-side contribution using (3.9) and the right-hand-side contribution using (3.10). The outcome reduces to

$$\Sigma_C(z,\boldsymbol{q},\boldsymbol{q}'')\,\mathbf{S}_0(\boldsymbol{q}'',\boldsymbol{q}') = -\int d\boldsymbol{q}'''\,L_{I+Q}(\boldsymbol{q},\boldsymbol{q}'')L_{I+Q}(\boldsymbol{q}',\boldsymbol{q}'')\,\mathbf{S}(z,\boldsymbol{q}\boldsymbol{q}'',\boldsymbol{q}'\boldsymbol{q}''') + \int d\boldsymbol{q}'''\,\Sigma(z,\boldsymbol{q},\boldsymbol{q}'')\,L_{I+Q}(\boldsymbol{q}',\boldsymbol{q}'')\,\mathbf{S}(z,\boldsymbol{q}'',\boldsymbol{q}'\boldsymbol{q}''') \tag{4.5}$$

after using (4.4). From (4.2) it follows formally that

$$\Sigma(z,\boldsymbol{q},\boldsymbol{q}'') = \int d\boldsymbol{q}'''\, L_{I+Q}(\boldsymbol{q},\boldsymbol{q}''') \times \mathbf{S}^{-1}(z,\boldsymbol{q}',\boldsymbol{q}'')\,\mathbf{S}(z,\boldsymbol{q}\boldsymbol{q}''',\boldsymbol{q}'). \quad (4.6)$$

Inserting (4.6) into the right-hand side of (4.5) and taking the $\boldsymbol{q}'$ integration on both sides yield

$$nf_0(p'')\,\Sigma_C(z,\boldsymbol{q},\boldsymbol{q}'') = -\int d\boldsymbol{q}''d\boldsymbol{q}'''\, L_{I+Q}(\boldsymbol{q},\boldsymbol{q}'')L_{I+Q} \times (\boldsymbol{q}',\boldsymbol{q}''')\,\mathbf{G}(z,\boldsymbol{q}\boldsymbol{q}'',\boldsymbol{q}'\boldsymbol{q}''') \quad (4.7)$$

with $\mathbf{G}$ a four-point phase-space correlation function

$$\mathbf{G}(z,\boldsymbol{q}\boldsymbol{q}_1',\boldsymbol{q}'\boldsymbol{q}_2') = \mathbf{S}(z,\boldsymbol{q}\boldsymbol{q}_1',\boldsymbol{q}'\boldsymbol{q}_2') - \int d\boldsymbol{q}_3 d\boldsymbol{q}_4 \mathbf{S}(z,\boldsymbol{q}\boldsymbol{q}_1',\boldsymbol{q}_3) \times \mathbf{S}^{-1}(z,\boldsymbol{q}_3,\boldsymbol{q}_4)\mathbf{S}(z,\boldsymbol{q}_4,\boldsymbol{q}'\boldsymbol{q}_2'). \quad (4.8)$$

The collisional character of the self-energy Σ_C is manifest in (4.7). The formal relation for the collisional self-energy (4.7) was initially derived in [13,14] for the one-component and Abelian-Coulomb plasma. We now have shown that it holds for any non-Abelian SU(N) Coulomb plasma.

Equation (4.7) shows that the connected part of the self-energy kernel is actually tied to a four-point correlator in the colored phase space. In terms of (4.7), the original kinetic equation (3.7) now reads

$$[z - L_0(\boldsymbol{q})]\mathbf{S}(z,\boldsymbol{q},\boldsymbol{q}') - \int d\boldsymbol{q}''\Sigma_S(\boldsymbol{q},\boldsymbol{q}'')\mathbf{S}(z,\boldsymbol{q}'',\boldsymbol{q}') = \mathbf{S}_0(\boldsymbol{q},\boldsymbol{q}') - \int d\boldsymbol{q}''\, d\boldsymbol{q}_1 d\boldsymbol{q}_2\, L_{I+Q}(\boldsymbol{q},\boldsymbol{q}_1)L_{I+Q}(\boldsymbol{q}'',\boldsymbol{q}_2) \times \mathbf{G}(z,\boldsymbol{q}\boldsymbol{q}_1,\boldsymbol{q}''\boldsymbol{q}_2)\,\mathbf{S}(z,\boldsymbol{q}'',\boldsymbol{q}'), \quad (4.9)$$

which is a Boltzmann-like equation. The key difference is that it involves correlation functions and the Boltzmann-like kernel in the right-hand side is *not* a scattering amplitude but rather a reduced four-point correlation function. Equation (4.9) reduces to the Boltzmann equation for weak coupling. An alternative derivation of (4.9) can be found in Appendix C through a direct projection of (4.2) in phase space.

V. FREE-STREAMING APPROXIMATION

The formal kinetic equation (4.7) can be closed by approximating the four-point correlation function in the color phase space by a product of two-point correlation function [14],

$$\mathbf{G}(t,\boldsymbol{q}\boldsymbol{q}_1,\boldsymbol{q}'\boldsymbol{q}_2) \approx [\mathbf{S}(t,\boldsymbol{q},\boldsymbol{q}')\mathbf{S}(t,\boldsymbol{q}_1,\boldsymbol{q}_2) + \mathbf{S}(t,\boldsymbol{q},\boldsymbol{q}_2)\mathbf{S}(t,\boldsymbol{q}',\boldsymbol{q}_1)]. \quad (5.1)$$

This reduction will be referred to as the free-steaming approximation. Next we substitute the colored Coulomb potentials in the double Liouville operator $L_{I+Q}\times L_{I+Q}$ with a bare Coulomb $\mathbf{V}(\boldsymbol{r}-\boldsymbol{r}',\boldsymbol{Q}\cdot\boldsymbol{Q}') = \boldsymbol{Q}\cdot\boldsymbol{Q}'/|\boldsymbol{r}-\boldsymbol{r}'|$,

$$L_{I+Q}(\boldsymbol{q},\boldsymbol{q}_1) = i\nabla_r\mathbf{V}(\boldsymbol{r}-\boldsymbol{r}_1,\boldsymbol{Q}\cdot\boldsymbol{Q}_1)\cdot(\nabla_p-\nabla_{p_1}) - i\big[\boldsymbol{Q}\times\nabla_Q\mathbf{V}(\boldsymbol{r}-\boldsymbol{r}_1,\boldsymbol{Q}\cdot\boldsymbol{Q}_1)\cdot\nabla_Q + \boldsymbol{Q}_1\times\nabla_{Q_1}\mathbf{V}(\boldsymbol{r}-\boldsymbol{r}_1,\boldsymbol{Q}\cdot\boldsymbol{Q}_1)\cdot\nabla_{Q_1}\big] \quad (5.2)$$

times a dressed colored Coulomb potential $\mathbf{c}_D$ defined in [10]

$$L^R_{I+Q}(\boldsymbol{q},\boldsymbol{q}_1) = -i\frac{1}{\beta}\nabla_r\mathbf{c}_D(\boldsymbol{r}-\boldsymbol{r}_1,\boldsymbol{Q}\cdot\boldsymbol{Q}_1)\cdot(\nabla_p-\nabla_{p_1}) + i\frac{1}{\beta}\big[\boldsymbol{Q}\times\nabla_Q\mathbf{c}_D(\boldsymbol{r}-\boldsymbol{r}_1,\boldsymbol{Q}\cdot\boldsymbol{Q}_1)\cdot\nabla_Q + \boldsymbol{Q}_1\times\nabla_{Q_1}\mathbf{c}_D(\boldsymbol{r}-\boldsymbol{r}_1,\boldsymbol{Q}\cdot\boldsymbol{Q}_1)\cdot\nabla_{Q_1}\big]. \quad (5.3)$$

This bare-dressed or half renormalization was initially suggested [15] in the context of the one-component Coulomb plasma to overcome the shortcomings of a full or dressed-dressed renormalization initially suggested in [13,14]. The latter was shown to upset the initial conditions. Thus

$$L_{I+Q}(\boldsymbol{q},\boldsymbol{q}_1)L_{I+Q}(\boldsymbol{q}',\boldsymbol{q}_2) \to \tfrac{1}{2}\big[L_{I+Q}(\boldsymbol{q},\boldsymbol{q}_1)L^R_{I+Q}(\boldsymbol{q}',\boldsymbol{q}_2) + L^R_{I+Q}(\boldsymbol{q},\boldsymbol{q}_1)L_{I+Q}(\boldsymbol{q}',\boldsymbol{q}_2)\big]. \quad (5.4)$$

Combining (5.1) and (5.4) in (4.7) yields

$$n\,f_0(\boldsymbol{p}')\,\Sigma_C(t,\boldsymbol{q},\boldsymbol{q}') \approx -\frac{1}{2}\int d\boldsymbol{q}_1\, d\boldsymbol{q}_2\,\big[L_{I+Q}(\boldsymbol{q},\boldsymbol{q}_1)L^R_{I+Q}(\boldsymbol{q}',\boldsymbol{q}_2)\mathbf{S}(t,\boldsymbol{q},\boldsymbol{q}') \times\mathbf{S}(t,\boldsymbol{q}_1,\boldsymbol{q}_2) + L_{I+Q}(\boldsymbol{q},\boldsymbol{q}_1)L^R_{I+Q}(\boldsymbol{q}',\boldsymbol{q}_2)\mathbf{S}(t,\boldsymbol{q},\boldsymbol{q}_2) \times\mathbf{S}(t,\boldsymbol{q}',\boldsymbol{q}_1) + (\boldsymbol{q}_1\leftrightarrow\boldsymbol{q}_2,\boldsymbol{q}\leftrightarrow\boldsymbol{q}')\big]. \quad (5.5)$$

This is the half-dressed but free-streaming approximation for the connected part of the self-energy for the colored Coulomb plasma. Translational invariance in space and rotational invariance in color space allows a further reduction of (5.5) by Fourier and Legendre transforms, respectively. Indeed, Eq. (5.5) yields

$$\begin{aligned} n\,f_0(\boldsymbol{p}')\,\Sigma_C(t,\boldsymbol{q},\boldsymbol{q}') &\approx -\frac{1}{2}\int d\boldsymbol{q}_1\, d\boldsymbol{q}_2\,\big[L_I(\boldsymbol{q},\boldsymbol{q}_1)L^R_I(\boldsymbol{q}',\boldsymbol{q}_2)\mathbf{S}(t,\boldsymbol{q},\boldsymbol{q}')\mathbf{S}(t,\boldsymbol{q}_1,\boldsymbol{q}_2) \\ &\quad + L_I(\boldsymbol{q},\boldsymbol{q}_1)L^R_I(\boldsymbol{q}',\boldsymbol{q}_2)\mathbf{S}(t,\boldsymbol{q},\boldsymbol{q}_2)\mathbf{S}(t,\boldsymbol{q}',\boldsymbol{q}_1) + (\boldsymbol{q}_1\leftrightarrow\boldsymbol{q}_2,\boldsymbol{q}\leftrightarrow\boldsymbol{q}')\big] \\ &= -\frac{1}{2\beta}\int d\boldsymbol{q}_1\, d\boldsymbol{q}_2\,[\nabla_r\mathbf{c}_D(\boldsymbol{r}-\boldsymbol{r}_1,\boldsymbol{Q}\cdot\boldsymbol{Q}_1)\cdot\nabla_p\nabla_{r'}\mathbf{V}(\boldsymbol{r}'-\boldsymbol{r}_2,\boldsymbol{Q}'\cdot\boldsymbol{Q}_2)\cdot\nabla_{p'}\mathbf{S}(t,\boldsymbol{q},\boldsymbol{q}')\mathbf{S}(t,\boldsymbol{q}_1,\boldsymbol{q}_2) \\ &\quad + \nabla_r\mathbf{c}_D(\boldsymbol{r}-\boldsymbol{r}_1,\boldsymbol{Q}\cdot\boldsymbol{Q}_1)\cdot\nabla_p\nabla_{r'}\mathbf{V}(\boldsymbol{r}'-\boldsymbol{r}_2,\boldsymbol{Q}'\cdot\boldsymbol{Q}_2)\cdot\nabla_{p'}\mathbf{S}(t,\boldsymbol{q},\boldsymbol{q}_2)\mathbf{S}(t,\boldsymbol{q}',\boldsymbol{q}_1) + (\boldsymbol{q}_1\leftrightarrow\boldsymbol{q}_2,\boldsymbol{q}\leftrightarrow\boldsymbol{q}')], \end{aligned} \quad (5.6)$$

where we note that the colored part of the Liouville operator dropped from the collision kernel in the free-streaming approximation as we detail in Appendix C. Both sides of (5.6) can be now Legendre transformed in color

to give

$$
\begin{aligned}
& n\, f_0(\boldsymbol{p}') \sum_l \Sigma_{Cl}(t, \boldsymbol{r}\boldsymbol{r}', \boldsymbol{p}\boldsymbol{p}') \frac{2l+1}{4\pi} P_l(\boldsymbol{Q}\cdot\boldsymbol{Q}') \\
& \approx -\frac{1}{2\beta}\int d\boldsymbol{r}_1 d\boldsymbol{p}_1 d\boldsymbol{r}_2 d\boldsymbol{p}_2 \sum_l \frac{2l+1}{4\pi}\left(\frac{l+1}{2l+1}P_{l+1}(\boldsymbol{Q}\cdot\boldsymbol{Q}') + \frac{l}{2l+1}P_{l-1}(\boldsymbol{Q}\cdot\boldsymbol{Q}')\right) \\
& \times \Bigg(\nabla_r \mathbf{c}_{D1}(\boldsymbol{r}-\boldsymbol{r}_1)\cdot\nabla_p\nabla_{r'}\frac{1}{|\boldsymbol{r}'-\boldsymbol{r}_2|}\cdot\nabla_{p'}\mathbf{S}_l(t,\boldsymbol{r}\boldsymbol{r}',\boldsymbol{p}\boldsymbol{p}')\mathbf{S}_1(t,\boldsymbol{r}_1\boldsymbol{r}_2,\boldsymbol{p}_1\boldsymbol{p}_2) \\
& + \nabla_r \mathbf{c}_{Dl}(\boldsymbol{r}-\boldsymbol{r}_1)\cdot\nabla_p\nabla_{r'}\frac{1}{|\boldsymbol{r}'-\boldsymbol{r}_2|}\cdot\nabla_{p'}\mathbf{S}_1(t,\boldsymbol{r}\boldsymbol{r}_2,\boldsymbol{p}\boldsymbol{p}_2)\mathbf{S}_l(t,\boldsymbol{r}'\boldsymbol{r}_1,\boldsymbol{p}'\boldsymbol{p}_1) \\
& + \nabla_{r'} \mathbf{c}_{Dl}(\boldsymbol{r}'-\boldsymbol{r}_2)\cdot\nabla_{p'}\nabla_{r}\frac{1}{|\boldsymbol{r}-\boldsymbol{r}_1|}\cdot\nabla_{p}\mathbf{S}_l(t,\boldsymbol{r}\boldsymbol{r}_2,\boldsymbol{p}\boldsymbol{p}_2)\mathbf{S}_1(t,\boldsymbol{r}'\boldsymbol{r}_1,\boldsymbol{p}'\boldsymbol{p}_1) \\
& + \nabla_{r'} \mathbf{c}_{D1}(\boldsymbol{r}'-\boldsymbol{r}_2)\cdot\nabla_{p'}\nabla_{r}\frac{1}{|\boldsymbol{r}-\boldsymbol{r}_1|}\cdot\nabla_{p}\mathbf{S}_l(t,\boldsymbol{r}\boldsymbol{r}',\boldsymbol{p}\boldsymbol{p}')\mathbf{S}_1(t,\boldsymbol{r}_1\boldsymbol{r}_2,\boldsymbol{p}_1\boldsymbol{p}_2)\Bigg).
\end{aligned}
\tag{5.7}
$$

Thus

$$
\begin{aligned}
n\, f_0(\boldsymbol{p}')\,\Sigma_{Cl}(t,\boldsymbol{r}\boldsymbol{r}',\boldsymbol{p}\boldsymbol{p}') \approx & -\frac{1}{2\beta}\int d\boldsymbol{r}_1 d\boldsymbol{p}_1 d\boldsymbol{r}_2 d\boldsymbol{p}_2 \Bigg[\nabla_r \mathbf{c}_{D1}(\boldsymbol{r}-\boldsymbol{r}_1)\cdot\nabla_p\nabla_{r'}\frac{1}{|\boldsymbol{r}'-\boldsymbol{r}_2|}\cdot\nabla_{p'} \\
& \times\left(\frac{l}{2l+1}\mathbf{S}_{l-1}(t,\boldsymbol{r}\boldsymbol{r}',\boldsymbol{p}\boldsymbol{p}')\mathbf{S}_1(t,\boldsymbol{r}_1\boldsymbol{r}_2,\boldsymbol{p}_1\boldsymbol{p}_2) + \frac{l+1}{2l+1}\mathbf{S}_{l+1}(t,\boldsymbol{r}\boldsymbol{r}',\boldsymbol{p}\boldsymbol{p}')\mathbf{S}_1(t,\boldsymbol{r}_1\boldsymbol{r}_2,\boldsymbol{p}_1\boldsymbol{p}_2)\right) \\
& + \nabla_r \mathbf{c}_{D1}(\boldsymbol{r}-\boldsymbol{r}_1)\cdot\nabla_p\nabla_{r'}\frac{1}{|\boldsymbol{r}'-\boldsymbol{r}_2|}\cdot\nabla_{p'} \\
& \times\left(\frac{l}{2l+1}\mathbf{S}_1(t,\boldsymbol{r}\boldsymbol{r}_2,\boldsymbol{p}\boldsymbol{p}_2)\mathbf{S}_{l-1}(t,\boldsymbol{r}'\boldsymbol{r}_1,\boldsymbol{p}'\boldsymbol{p}_1) + \frac{l+1}{2l+1}\mathbf{S}_1(t,\boldsymbol{r}\boldsymbol{r}_2,\boldsymbol{p}\boldsymbol{p}_2)\mathbf{S}_{l+1}(t,\boldsymbol{r}'\boldsymbol{r}_1,\boldsymbol{p}'\boldsymbol{p}_1)\right) \\
& + \nabla_{r'} \mathbf{c}_{Dl}(\boldsymbol{r}'-\boldsymbol{r}_2)\cdot\nabla_{p'}\nabla_{r}\frac{1}{|\boldsymbol{r}-\boldsymbol{r}_1|}\cdot\nabla_{p} \\
& \times\left(\frac{l}{2l+1}\mathbf{S}_{l-1}(t,\boldsymbol{r}\boldsymbol{r}_2,\boldsymbol{p}\boldsymbol{p}_2)\mathbf{S}_1(t,\boldsymbol{r}'\boldsymbol{r}_1,\boldsymbol{p}'\boldsymbol{p}_1) + \frac{l+1}{2l+1}\mathbf{S}_{l+1}(t,\boldsymbol{r}\boldsymbol{r}_2,\boldsymbol{p}\boldsymbol{p}_2)\mathbf{S}_1(t,\boldsymbol{r}'\boldsymbol{r}_1,\boldsymbol{p}'\boldsymbol{p}_1)\right) \\
& + \nabla_{r'} \mathbf{c}_{D1}(\boldsymbol{r}'-\boldsymbol{r}_2)\cdot\nabla_{p'}\nabla_{r}\frac{1}{|\boldsymbol{r}-\boldsymbol{r}_1|}\cdot\nabla_{p} \\
& \times\left(\frac{l}{2l+1}\mathbf{S}_{l-1}(t,\boldsymbol{r}\boldsymbol{r}',\boldsymbol{p}\boldsymbol{p}')\mathbf{S}_1(t,\boldsymbol{r}_1\boldsymbol{r}_2,\boldsymbol{p}_1\boldsymbol{p}_2) + \frac{l+1}{2l+1}\mathbf{S}_{l+1}(t,\boldsymbol{r}\boldsymbol{r}',\boldsymbol{p}\boldsymbol{p}')\mathbf{S}_1(t,\boldsymbol{r}_1\boldsymbol{r}_2,\boldsymbol{p}_1\boldsymbol{p}_2)\right)\Bigg]
\end{aligned}
\tag{5.8}
$$

with $\mathbf{S}_{l-1}\equiv 0$ by definition. In the colored Coulomb plasma the collisional contributions diagonalize in the color projected channels labeled by l, with $l=0$ being the density channel, $l=1$ the plasmon channel, and so on. In momentum space (5.8) reads

$$
\begin{aligned}
n\, f_0(\boldsymbol{p}')\,\Sigma_{Cl}(t,\boldsymbol{k},\boldsymbol{p}\boldsymbol{p}') = & -\frac{1}{2\beta}\int d\boldsymbol{p}_1 d\boldsymbol{p}_2 \int\frac{d\boldsymbol{l}}{(2\pi)^3}\Bigg[\boldsymbol{l}\cdot\nabla_p\boldsymbol{l}\cdot\nabla_{p'}\mathbf{c}_{D1}(l)V_l \\
& \times\left(\frac{l}{2l+1}\mathbf{S}_{l-1}(t,\boldsymbol{k}-\boldsymbol{l},\boldsymbol{p}\boldsymbol{p}')\mathbf{S}_1(t,\boldsymbol{l},\boldsymbol{p}_1\boldsymbol{p}_2) + \frac{l+1}{2l+1}\mathbf{S}_{l+1}(t,\boldsymbol{k}-\boldsymbol{l},\boldsymbol{p}\boldsymbol{p}')\mathbf{S}_1(t,\boldsymbol{l},\boldsymbol{p}_1\boldsymbol{p}_2)\right) \\
& + \boldsymbol{l}\cdot\nabla_p(\boldsymbol{k}-\boldsymbol{l})\cdot\nabla_{p'}\mathbf{c}_{Dl}(l)V_{k-l} \\
& \times\left(\frac{l}{2l+1}\mathbf{S}_1(t,\boldsymbol{k}-\boldsymbol{l},\boldsymbol{p}\boldsymbol{p}_2)\mathbf{S}_{l-1}(t,\boldsymbol{l},\boldsymbol{p}'\boldsymbol{p}_1) + \frac{l+1}{2l+1}\mathbf{S}_1(t,\boldsymbol{k}-\boldsymbol{l},\boldsymbol{p}\boldsymbol{p}_2)\mathbf{S}_{1+1}(t,\boldsymbol{l},\boldsymbol{p}'\boldsymbol{p}_1)\right) \\
& + (\boldsymbol{k}-\boldsymbol{l})\cdot\nabla_p\boldsymbol{l}\cdot\nabla_{p'}\mathbf{c}_{Dl}(l)V_{k-l} \\
& \times\left(\frac{l}{2l+1}\mathbf{S}_{l-1}(t,\boldsymbol{l},\boldsymbol{p}\boldsymbol{p}_2)\mathbf{S}_l(t,\boldsymbol{k}-\boldsymbol{l},\boldsymbol{p}'\boldsymbol{p}_1) + \frac{l+1}{2l+1}\mathbf{S}_{l+1}(t,\boldsymbol{l},\boldsymbol{p}\boldsymbol{p}_2)\mathbf{S}_1(t,\boldsymbol{k}-\boldsymbol{l},\boldsymbol{p}'\boldsymbol{p}_1)\right) \\
& + \boldsymbol{l}\cdot\nabla_p\boldsymbol{l}\cdot\nabla_{p'}\mathbf{c}_{D1}(l)V_l \\
& \times\left(\frac{l}{2l+1}\mathbf{S}_{l-1}(t,\boldsymbol{k}-\boldsymbol{l},\boldsymbol{p}\boldsymbol{p}')\mathbf{S}_1(t,\boldsymbol{l},\boldsymbol{p}_1\boldsymbol{p}_2) + \frac{l+1}{2l+1}\mathbf{S}_{l+1}(t,\boldsymbol{k}-\boldsymbol{l},\boldsymbol{p}\boldsymbol{p}')\mathbf{S}_1(t,\boldsymbol{l},\boldsymbol{p}_1\boldsymbol{p}_2)\right)\Bigg]
\end{aligned}
\tag{5.9}
$$

with $V_l = 4\pi/\boldsymbol{l}^2$. We note that for $l=0$ which is the colorless density channel (5.9) involves only $\mathbf{S}_1$ which is the time-dependent charged form factor due to the Coulomb interactions.

VI. HYDRODYNAMICAL PROJECTION

In terms of (5.9), (4.2), and

$$\Sigma_l(z\boldsymbol{k},\,\boldsymbol{p}\boldsymbol{p}_1)=(\Sigma_{0l}+\Sigma_{Il}+\Sigma_{Ql}+\Sigma_{Cl})(z\boldsymbol{k},\,\boldsymbol{p}\boldsymbol{p}_1), \tag{6.1}$$

the Fourier and Legendre transform of the kinetic equation (3.7) now reads

$$z\mathbf{S}_l(z\boldsymbol{k},\,\boldsymbol{p}\boldsymbol{p}')-\int d\boldsymbol{p}_1\,\Sigma_l(z\boldsymbol{k},\,\boldsymbol{p}\boldsymbol{p}_1)\mathbf{S}_l(z\boldsymbol{k},\,\boldsymbol{p}_1\boldsymbol{p}') = \mathbf{S}_{0l}(\boldsymbol{k},\,\boldsymbol{p}\boldsymbol{p}') \tag{6.2}$$

with $\Sigma_{0l}=L_0$ and $\Sigma_{Sl}=L_{(I+Q)l}$. Specifically

$$\begin{aligned}\Sigma_{0l}(z\boldsymbol{k},\,\boldsymbol{p}\boldsymbol{p}_1)&=\boldsymbol{k}\cdot\boldsymbol{v}\delta(\boldsymbol{p}-\boldsymbol{p}_1),\\ \Sigma_{Il}(z\boldsymbol{k},\,\boldsymbol{p}\boldsymbol{p}_1)&=-n\,f_0(p)\frac{\boldsymbol{k}\cdot\boldsymbol{p}}{m}\,\mathbf{c}_{Dl}(\boldsymbol{k}),\\ \Sigma_{Ql}(z\boldsymbol{k},\,\boldsymbol{p}\boldsymbol{p}_1)&=0,\end{aligned} \tag{6.3}$$

and Σ_{Cl} is defined in (5.9). See also Appendix B for an alternative but equivalent derivation using the operator projection method.

Equation (6.2) is the key kinetic equation for the colored Coulomb plasma. It still contains considerable information in phase space. A special limit of the classical phase space is the long wavelength or hydrodynamical limit. In this limit, only a few moments of the phase-space fluctuations δf or equivalently their correlations in $\mathbf{S}\approx\langle\delta f\,\delta f\rangle$ will be of interest. In particular,

$$\begin{aligned}\boldsymbol{n}(t,\boldsymbol{r})&=\int d\boldsymbol{p}d\boldsymbol{Q}\,\delta f(t,\boldsymbol{r},\,\boldsymbol{p},\,\boldsymbol{Q}),\\ \boldsymbol{p}(t,\boldsymbol{r})&=\int d\boldsymbol{p}d\boldsymbol{Q}\,\boldsymbol{p}\,\delta f(t,\boldsymbol{r},\,\boldsymbol{p},\,\boldsymbol{Q}),\\ \mathbf{e}(t,\boldsymbol{r})&=\int d\boldsymbol{p}d\boldsymbol{Q}\,\frac{p^2}{2m}\,\delta f(t,\boldsymbol{r},\,\boldsymbol{p},\,\boldsymbol{Q}),\end{aligned} \tag{6.4}$$

the local particle density, three-momentum, and energy (kinetic). The hydrodynamical sector described by the macrovariables (6.4) is colorless. An interesting macrovariable which carries charge representation of SU(2) would be

$$\mathbf{n}_l(t,\boldsymbol{r})=\frac{1}{2l+1}\sum_m\int d\boldsymbol{r}d\boldsymbol{Q}\,Y_l^m(\boldsymbol{Q})\,\delta f(t,\boldsymbol{r},\,\boldsymbol{p},\,\boldsymbol{Q}) \tag{6.5}$$

which reduces to the l color density with $l=0$ being the particle density, $l=1$ the charged color monopole density, $l=2$ the charged color quadrupole density, and so on. Because of color rotational invariance in the SU(2) colored Coulomb plasma, the constitutive equations for (6.5) which amount to charge conservation hold for each l.

To project (6.2) onto the hydrodynamical part of the phase space characterized by (6.5) and (6.4), we define the hydrodynamical projectors

$$\mathcal{P}_H=\sum_{i=1}^{5}|i\rangle\langle i|,\quad \mathcal{Q}_H=\mathbf{1}_H-\mathcal{P}_H, \tag{6.6}$$

with $1=$ density, $2,4,5=$ momentum, and $3=$ energy as detailed in Appendix D. When the $l=0$ particle density is retained in (6.6) the projection is on the colorless sector of the phase space. When the $l=1$ charged monopole density is retained in (6.6) the projection is on the plasmon channel, and so on. Most of the discussion to follow will focus on projecting on the canonical hydrodynamical phase space (6.4) with $l=0$ or singlet representation. The inclusion of the $l\neq 0$ representations of SU(2) is straightforward.

Formally (6.1) can be viewed as a $\boldsymbol{p}\times\boldsymbol{p}_1$ matrix in momentum space

$$[z-\Sigma_l(z\boldsymbol{k})]\;\mathbf{S}_l(z\boldsymbol{k})=\mathbf{S}_{0l}(\boldsymbol{k}). \tag{6.7}$$

The projection of the matrix equation (6.7) follows the same procedure as in Appendix B. The result is

$$\begin{aligned}&[z-\mathcal{P}_H\Sigma_l(z\boldsymbol{k})\mathcal{P}_H-\mathcal{P}_H\Theta_l(z\boldsymbol{k})\mathcal{P}_H]\,\mathcal{P}_H\mathbf{S}_l(z\boldsymbol{k})\mathcal{P}_H\\ &\quad=\mathcal{P}_H\mathbf{S}_{0l}(k)\mathcal{P}_H\end{aligned} \tag{6.8}$$

with

$$\Theta_l=\Sigma_l(z\boldsymbol{k})\mathcal{Q}_H[z-\mathcal{Q}_H\Sigma_H(z\boldsymbol{k})\mathcal{Q}_H]^{-1}\mathcal{Q}_H\Sigma_l(z\boldsymbol{k}). \tag{6.9}$$

If we define the hydrodynamical matrix elements

$$\begin{aligned}\mathbf{G}_{lij}(z\boldsymbol{k})&=\langle i|\mathbf{S}_l(z\boldsymbol{k})|j\rangle,\\ \Sigma_{lij}(z\boldsymbol{k})&=\langle i|\Sigma_l(z\boldsymbol{k})|j\rangle,\\ \Theta_{lij}(z\boldsymbol{k})&=\langle i|\Theta_l(z\boldsymbol{k})|j\rangle,\\ \mathbf{G}_{0lij}(z\boldsymbol{k})&=\langle i|\mathbf{S}_{0l}(\boldsymbol{k})|j\rangle,\end{aligned} \tag{6.10}$$

then (6.8) reads

$$[z\delta_{ii'}-\Omega_{lij}(z\boldsymbol{k})]\,\mathbf{G}_{lji'}(z\boldsymbol{k})=\mathbf{G}_{0lii'}(\boldsymbol{k}) \tag{6.11}$$

with $\Omega_l=\Sigma_l+\Theta_l$. Equation (6.11) takes the form of a dispersion for each color partial wave l with the projection operator (6.6) set by the pertinent density (6.5). The contribution Σ_l to Ω_l will be referred to as *direct* while the contribution Θ_l will be referred to as *indirect*.

VII. HYDRODYNAMICAL MODES

The zeros of (6.11) are the hydrodynamical modes originating from the Liouville equation for the time-dependent structure factor. The equation is closed under the free-streaming approximation with half-renormalized vertices as we detailed above.

We start by analyzing the two transverse modes with $i=T$ in (6.10) and (6.11). We note with [16] that $\mathbf{G}_{lTi}=0$ whenever $T\neq i$. The hydrodynamical projection (see Appendix D) causes the integrand to be odd whatever l. The two independent transverse modes in (6.11) decouple from the longitudinal $i=L$, the (kinetic) energy $i=E$, and particle density $i=N$ modes for all color projections. Thus

$$\mathbf{G}_{lT}(z\boldsymbol{k})=\frac{1}{z-\Omega_{lT}(z\boldsymbol{k})}, \tag{7.1}$$

with $\Omega_{lT}=\langle T|\Omega_l|T\rangle$ and $\mathbf{G}_{lT}=\langle T|\mathbf{G}_l|T\rangle$. The hydroprojected time-dependent l structure factor for fixed frequency $z=\omega+i0$, wave number k develops two transverse poles

$$z_l(\boldsymbol{k})=\Omega_{lT}(z\boldsymbol{k})\approx\mathcal{O}(k^2). \tag{7.2}$$

The last estimate follows from O(3) momentum symmetry under statistical averaging whatever the color projection. We

identify the transverse poles in (7.2) with two shear modes of consititutive dispersion

$$\omega + i\frac{\eta_l}{mn}k^2 + \mathcal{O}(k^3) = 0 \tag{7.3}$$

with η_l the shear viscosity for the lth color representation. Unlike conventional plasmas, the classical SU(2) color Coulomb plasma admits an infinite hierarchy of shear modes for each representation l.

The remaining three hydrodynamical modes L, E, N are more involved as they mix in (6.11) and under general symmetry consideration. Indeed current conservation ties the L mode to the N mode, for instance. Most of the symmetry arguments regarding the generic nature of Ω_l in [16] carry to our case for each color representation. Thus, for the three remaining nontransverse modes (6.11) reads in matrix form

$$\begin{pmatrix} \mathbf{G}_{lNN} & \mathbf{G}_{lNL} & \mathbf{G}_{lNE} \\ \mathbf{G}_{lLN} & \mathbf{G}_{lLL} & \mathbf{G}_{lLE} \\ \mathbf{G}_{lEN} & \mathbf{G}_{lEL} & \mathbf{G}_{lEE} \end{pmatrix} = \begin{pmatrix} z & -\Omega_{lNL} & 0 \\ -\Omega_{lLN} & z-\Omega_{lLL} & -\Omega_{lLE} \\ 0 & -\Omega_{lEL} & z-\Omega_{lEE} \end{pmatrix}^{-1} \times \begin{pmatrix} 1+n\,\mathbf{h}_l & 0 & 0 \\ 0 & 1 & 0 \\ 0 & 0 & 1 \end{pmatrix}. \tag{7.4}$$

The three remaining hydrodynamical modes are the zeros of the determinant

$$\Delta_l = \begin{vmatrix} z & -\Omega_{lNL}(zk) & 0 \\ -\Omega_{lLN}(zk) & z-\Omega_{lLL}(zk) & -\Omega_{lLE}(zk) \\ 0 & -\Omega_{lEL}(zk) & z-\Omega_{lEE}(zk) \end{vmatrix} = 0. \tag{7.5}$$

(7.5) admits infinitly many solutions $z_l(k)$. We seek the hydrodynamical solutions as analytical solutions in k for small k, i.e., $z(k) = \sum_n z_{ln}k^n$ for each SU(2) color representation l. In leading order, we have

$$\Delta_l \approx z_{l0}\left(z_{l0}^2 - \frac{k^2T}{m}\,\mathbf{S}_{0l}^{-1}(k \approx 0)\right) \approx 0 \tag{7.6}$$

after using the symmetry properties of Ω_l as in [16] for each l. We have also made use of the generalized Ornstein-Zernicke equations for each l representation [10]. In Fig. 1 we show the molecular-dynamics simulation results for four typical structure factors [10],

$$\mathbf{S}_{0l}(\boldsymbol{k}) = \left(\frac{4\pi}{2l+1}\right)\left\langle\left|\sum_{jm} e^{i\boldsymbol{k}\cdot\boldsymbol{x}_j(0)}\,Y_l^m(\boldsymbol{Q}_i)\right|^2\right\rangle \tag{7.7}$$

for $l = 0, 1, 2, 3$. We have made use of the dimensionless wave number $q = k\,a_{\mathrm{WS}}$ with a_{WS} is the Wigner-Seitz radius. In Fig. 2 we show the analytical result for $\mathbf{S}_{01}$ which we will use for the numerical estimates below. We note that the $l = 1$ structure factor which amounts to the monopole structure

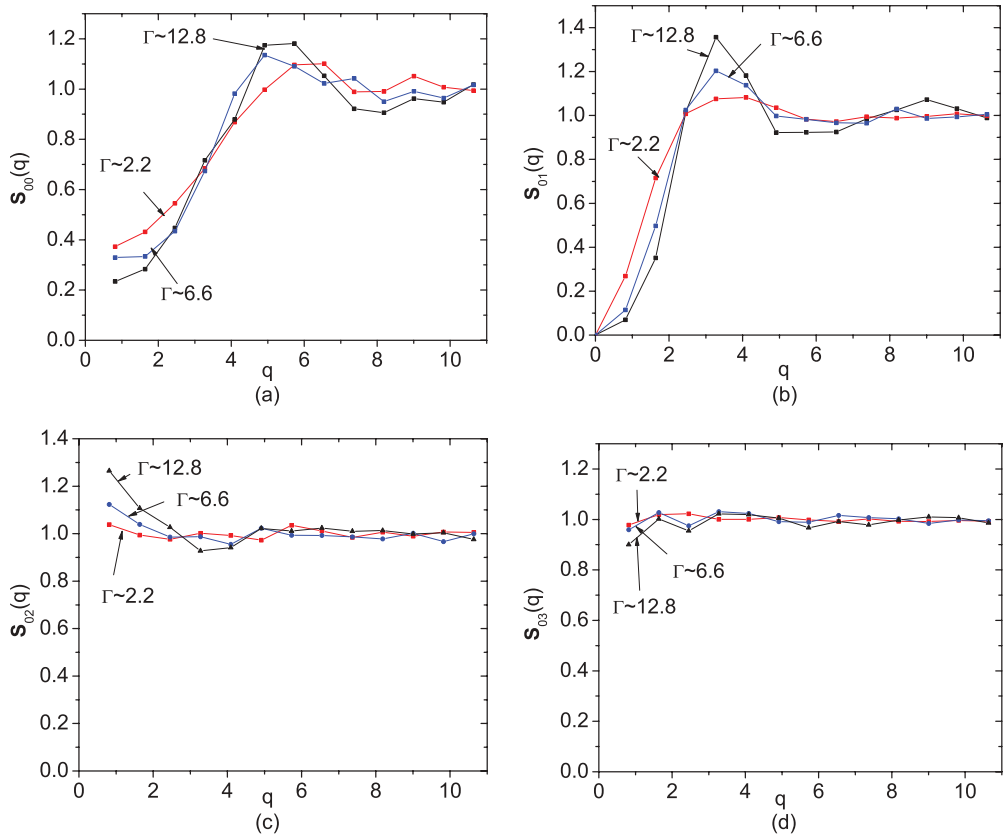

FIG. 1. (Color online) $\mathbf{S}_{0l}(q)$ from SU(2) molecular dynamics.

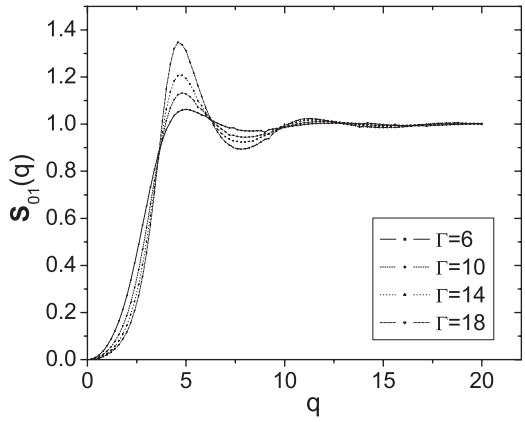

.

FIG. 2. $\mathbf{S}_{01}(q)$ for different Γ [10].

factor vanishes at $k = 0$. All other l's are finite at $k = 0$ with $l = 0$ corresponding to the density structure factor.

Equation (7.6) displays three hydrodynamical zeros as $k \to 0$ for each l representation. One is massless and we identify it with the diffusive heat mode. The molecular-dynamics simulations of the structure factors in Fig. 1 imply that all $l \neq 0$ channels are sound dominated with two massless modes, while the $l = 1$ is plasmon dominated with two massive longitudinal plasmon states. Thus

$$z_{l\pm} = \pm\omega_p^2 \delta_{l1} \tag{7.8}$$

with $\omega_p = k_D\sqrt{T/m}$ the plasmon frequency. The relevance of this channel to the energy loss has been discussed in [17]. We used $\mathbf{S}_{01}(k \approx 0) \approx k^2/k_D^2$ with k_D^2 the squared Debye momentum. All even $l \neq 1$ are contaminated by the sound modes. The SU(2) classical and colored Coulomb plasma supports plasmon oscillations even at strong coupling. These modes are important in the attenuation of soft monopole color oscillations.

VIII. SHEAR VISCOSITY

The transport parameters associated to the SU(2) classical and colored Coulomb plasma follows from the hydrodynamical projection and expansion discussed above. This includes the heat diffusion coefficient, the transverse shear viscosity, and the longitudinal plasmon frequency and damping parameters. In this section we discuss explicitly the shear viscosity coefficient for the SU(2) colored Coulomb plasma.

Throughout, we define $\lambda = \frac{4}{3}\pi(3\Gamma)^{3/2}$, the bare Coulomb interaction $\bar{V}_l = k_0^2/l^2$ in units of the Wigner-Seitz radius $k_0^{-1} = a_{\rm WS}$. While varying the Coulomb coupling

$$\Gamma = \frac{g^2}{4\pi}\beta\frac{C_2}{a_{\rm WS}} \tag{8.1}$$

all length scales will be measured in $a_{\rm WS} = (4\pi n/3)^{-1/3}$, all times in the inverse plasmon frequency $1/\omega_p$ with $\omega_p^2 = \kappa_D^2/m\beta = ng^2C_2/m$. All units of mass will be measured in m. The Debye momentum is $\kappa_D^2 = g^2n\beta C_2$ and the plasma density is n. For instance, the shear viscosity will be expressed in fixed dimensionless units of $\eta_0 = nm\omega_p a_{\rm WS}^2$.

The transverse shear viscosity follows from (7.1) with Σ_l contributing to the direct or hydrodynamical part, and Θ_l contributing to the indirect or single-particle part. For $l = 0$

$$\frac{\eta}{\eta_0} = \frac{\eta_{\rm dir}}{\eta_0} + \frac{\eta_{\rm ind}}{\eta_0}, \tag{8.2}$$

respectively. The direct or hydrodynamical contribution is likely to be dominant at strong coupling, while the indirect or single-particle contribution is likely to take over at weak coupling. We now proceed to show that.

The indirect contribution to the viscosity follows from the contribution outside the hydrodynamical subspace through $\mathcal{Q}_H$ and lumps the single-particle phase contributions. It involves the inversion of $\mathcal{Q}_H\Sigma_{C0}\mathcal{Q}_H$ in (B13) with

$$\begin{aligned}\eta_{\rm ind} &= \lim_{k\to 0}\frac{mn}{k^2}\frac{|\langle t|\Sigma_0|tl\rangle|^2}{\langle tl|i\Sigma_0|tl\rangle}\\ &= \lim_{k\to 0}\frac{mn}{k^2}\frac{|\langle t|(\Sigma_{00}+\Sigma_{C0})|tl\rangle|^2}{\langle tl|i\Sigma_{C0}|tl\rangle}.\end{aligned} \tag{8.3}$$

In short we expand Σ_{C0} in terms of generalized Hermite polynomials, with the first term identified with the stress tensor due to the projection operator (D3). The inversion follows by means of the first Sonine polynomial expansion. Explicitly

$$\begin{aligned}\eta^*_{\rm ind} &= \frac{\eta_{\rm ind}}{\eta_0} = nm\lim_{k\to 0}\frac{1}{k^2}\frac{|\langle t|\Sigma_{00}+\Sigma_{C0}(\boldsymbol{k},0)|lt\rangle|^2}{\langle lt|i\Sigma_{C0}(\boldsymbol{k},0)|lt\rangle}\\ &= \frac{(1+\lambda I_2)^2}{\lambda I_3}\end{aligned} \tag{8.4}$$

with

$$\begin{aligned}I_2 &= \frac{1}{60\pi^2}\frac{1}{(3\Gamma)^{1/2}}\int_0^\infty dq\{2[\mathbf{S}_{01}(q)^2-1]+[1-\mathbf{S}_{01}(q)]\},\\ I_3 &= \frac{1}{10\pi^{3/2}}\frac{1}{3\Gamma}\int_0^\infty dq\, q[1-\mathbf{S}_{01}(q)],\end{aligned} \tag{8.5}$$

with the dimensionless wave number $q = ka_{\rm WS}$.

We recall that $\mathbf{S}_{01}$ is the monopole structure factor discussed in [10] both analytically and numerically. In Fig. 2 we show the behavior of the static monopole structure factor from [10] for different Coulomb couplings. The larger Γ is the stronger the first peak, and the oscillations. These features characterize the onset of the crystalline structure in the SU(2) colored Coulomb plasma. A good fit to Fig. 2 follows from the following parametrization:

$$1 + C_0 e^{-q/C_1}\sin[(q-C_2)/C_3] \tag{8.6}$$

with four parameters $C_{0,1,2,3}$. The fit following from (8.6) extends to $q \approx 100$ within 10^{-5} accuracy, thanks to the exponent.

The direct contribution to the shear viscosity follows from similar arguments. From (7.1) and (7.3), we have in the zero-momentum limit

$$\eta_{\rm dir} = \lim_{k\to 0}\frac{mn}{k^2}\langle t|i\Sigma_0|t\rangle = \lim_{k\to 0}\frac{mn}{k^2}\langle t|i\Sigma_{C0}(0,0)|t\rangle \tag{8.7}$$

with $\Sigma_0 = \Sigma_{00} + \Sigma_{I0} + \Sigma_{C0}$ as defined in (6.3) and (5.9). Only those nonvanishing contributions after the

hydrodynamical projection were retained in the second equalities in (8.3) as we detail in Appendix D. A rerun of the arguments yields

$$\eta^*_{\rm dir} = \frac{\eta_{\rm dir}}{\eta_0} = \lambda \frac{\omega_p}{\kappa_D^3} \lim_{k\to 0} \frac{1}{\boldsymbol{k}^2} \int \frac{d\boldsymbol{l}}{(2\pi)^3} \int_0^\infty dt n(\boldsymbol{\epsilon}\cdot\boldsymbol{l})^2 \times [\mathbf{c}_{D1}(l)\mathcal{G}_{n1}(\boldsymbol{k}-\boldsymbol{l},t)\mathcal{G}_{n1}(\boldsymbol{l},t)\bar{V}_l - \mathbf{c}_{D0}(l)\mathcal{G}_{n1}(\boldsymbol{k}-\boldsymbol{l},t)\mathcal{G}_{n1}(\boldsymbol{l},t)\bar{V}_{k-l}]. \quad (8.8)$$

The projected nonstatic structure factor is

$$\mathcal{G}_{n1}(\boldsymbol{l},t) = \frac{1}{n}\int d\boldsymbol{p}\, d\boldsymbol{p}'\, \mathbf{S}_1(\boldsymbol{l},t;\boldsymbol{p}\boldsymbol{p}') = \overline{\mathcal{G}}_{n1}(\boldsymbol{l},t)\,\mathbf{S}_{01}(\boldsymbol{l}) \quad (8.9)$$

with the normalization $\overline{\mathcal{G}}_{n1}(\boldsymbol{l},0) = 1$. As in the one-component Coulomb plasma studied in [18] we will approximate the dynamical part by its intermediate time behavior where the motion is free. This consists in solving (4.1) with no self-energy kernel or $\Sigma = 0$,

$$\mathcal{G}_{n1}(\boldsymbol{l},t) \approx e^{-(lt)^2/2m\beta}\,\mathbf{S}_{01}(\boldsymbol{l}). \quad (8.10)$$

Thus inserting (8.10) and performing the integrations with $k \to 0$ yield the direct contribution to the shear viscosity

$$\eta^*_{\rm dir} = \frac{\eta_{\rm dir}}{\eta_0} = \frac{\sqrt{3}}{45\pi^{1/2}}\Gamma^{\frac{1}{2}}. \quad (8.11)$$

The full shear viscosity result is then

$$\eta^* = \frac{\eta}{\eta_0} = \frac{\eta_{\rm dir}}{\eta_0} + \frac{\eta_{\rm ind}}{\eta_0} = \frac{\sqrt{3}}{45\pi^{1/2}}\Gamma^{\frac{1}{2}} + \frac{(1+\lambda I_2)^2}{\lambda I_3} \quad (8.12)$$

after inserting (8.4) and (8.11) in (8.2). The result (8.12) for the shear viscosity of the transverse sound mode is analogous to the result for the sound velocity in the one-component plasma derived initially in [15] with two differences: (i) the SU(2) Casimir in Γ; (ii) the occurrence of $\mathbf{S}_{01}$ instead of $\mathbf{S}_{00}$. Since $\mathbf{S}_{01}$ is plasmon dominated at low momentum, we conclude that the shear viscosity is dominated by rescattering against the SU(2) plasmon modes in the cQGP.

Using the fitted monopole structure factor (8.6) in (8.5) we can numerically assess (8.4) for different values of Γ. Combining this result for the indirect viscosity together with (8.11) for the direct viscosity yield the colorless or sound viscosity η^*. The values of η^* are displayed in Table I and shown in Fig. 3 (solid line). The SU(2) molecular-dynamics simulations in [3], which are parametrized as

$$\eta^*_{\rm MD} \simeq 0.001\Gamma + \frac{0.242}{\Gamma^{0.3}} + \frac{0.072}{\Gamma^2}, \quad (8.13)$$

are also displayed in Table I and shown in Fig. 3 (dotted line) for comparison. The sound viscosity dips at about $\Gamma \approx 8$ in our analytical estimate. To understand the origin of the minimum, we display in Fig. 4 the scaling with Γ of the direct or hydrodynamical and the indirect part of the shear viscosity. The direct contribution to the viscosity grows like $\Gamma^{1/2}$; the indirect contribution drops like $1/\Gamma^{5/2}$. The latter dominates at weak coupling, while the former dominates at strong coupling. This is indeed expected, since the direct part is the contribution from the hydrodynamical part of the phase space, while the indirect part is the contribution from the nonhydrodynamical or single-particle part of phase space. The crossing is at $\Gamma \approx 4$.

TABLE I. Reduced shear viscosity. See the text.

Γ	2	4	6	8	10	12	14	16	18
$\eta^*_{\rm QGP}$	0.286	0.092	0.067	0.066	0.070	0.076	0.081	0.087	0.092
$\eta_{\rm MD}$	0.217	0.168	0.168	0.139	0.132	0.127	0.124	0.122	0.120

The reduced sound viscosity η_* is dimensionless. To restore dimensionality and compare with expectations for an SU(2) colored Coulomb plasma, we first note that the particle density is about $3 \times 0.244\, T^3 = 0.732\, T^3$. There are three physical gluons, each carrying blackbody density. The corresponding Wigner-Seitz radius is then $a_{\rm WS} = (3/4\pi n)^{1/3} \approx 0.688/T$. The Coulomb coupling is $\Gamma \approx 1.453\,(g^2N_c/4\pi)$. Since the plasmon frequency is $\omega_p^2 = \kappa_D^2/m\beta = ng^2N_c/m$, we get $\omega_p^2 \simeq 3.066\, T^2(g^2N_c/4\pi)$ with $m \simeq 3T$. The unit of viscosity $\eta_0 = nm\omega_p a_{\rm WS}^2$ translates to $1.822\, T^3(g^2N_c/4\pi)^{1/2}$. In these units, the viscosity for the SU(2) cQGP dips at about 0.066 which is $\eta^*_{\rm QGP} \approx 0.066\,\eta_0 \approx 0.120\, T^3\,(g^2N_c/4\pi)^{1/2}$. Since the entropy in our case is $\sigma = 6\,(4\pi^2/90)T^3$, we have for the SU(2) ratio $\eta/\sigma|_{SU(2)} = 0.046\,(g^2N_c/4\pi)^{1/2}$. The minimum in the viscosity occurs at $\Gamma = 1.453\,(g^2N_c/4\pi) \approx 8$, so that $(g^2N_c/4\pi)^{1/2} \approx 2.347$. Thus, our shear viscosity to entropy ratio is $\eta/\sigma|_{\rm SU(2)} \simeq 0.107$. A rerun of these estimates for SU(3) yields $\eta/\sigma|_{\rm SU(3)} \simeq 0.078$ which is lower than the bound $\eta/\sigma = 1/4\pi \simeq 0.0795$ suggested from holography.

Here we assumed on phenomenological grounds that $m \approx 3T$ in the region $(1-3)T_c$ as motivated by lattice simulations [7].

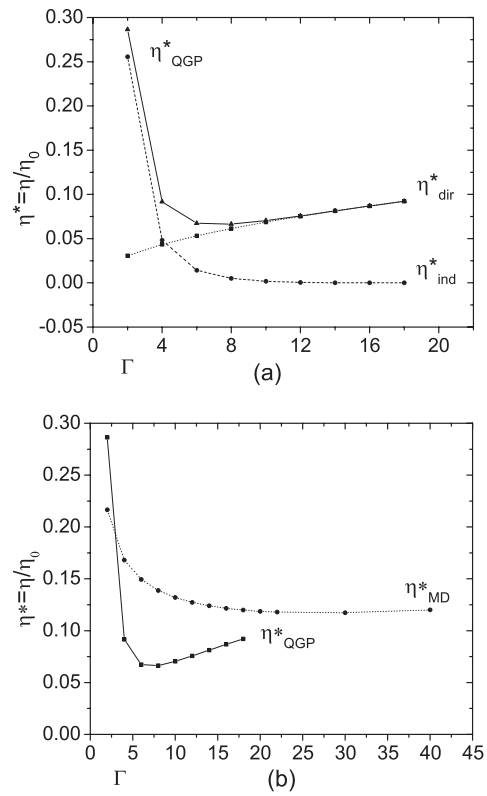

FIG. 3. The direct and indirect part of the viscosity.

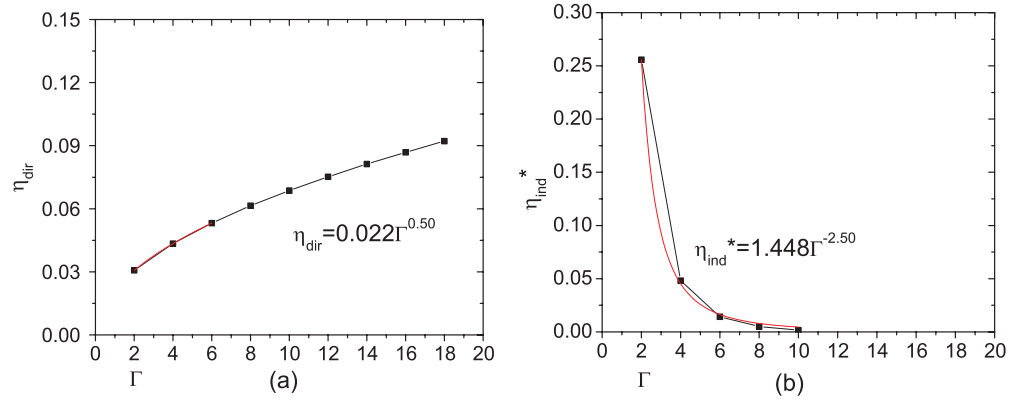

FIG. 4. (Color online) The best fit of the direct and indirect part of the viscosity.

Finally, we show the dimensionless shear viscosity $\eta*$ at low Γ (solid line) in Fig. 5(a) and large Γ (dotted line) in Fig. 5(b) assessed using the weak-coupling structure factor $S(k) = k^2/(k^2 + k_D^2)$. The discrepancy is noticeable for Γ near the liquid point. The large discrepancy for small values of Γ reflects on the fact that the integrals in (8.5) are infrared sensitive. The sensitivity is tamed by our analytical structure factor and the simulations. We recall that in weak coupling, the Landau viscosity η_L is [19]

$$\frac{\eta_L}{\eta_0} = \frac{5\sqrt{3\pi}}{18}\frac{1}{\Gamma^{5/2}}\frac{1}{\ln(r_D/r_0)}, \tag{8.14}$$

which follows from a mean-field analysis of the kinetic equation with the plasma dielectric constant set to 1. The logarithmic dependence in (8.14) reflects on the infrared and ultraviolet sensitivity of the mean-field approximation. Typically $r_D = 1/k_D$ and $r_0 = (g^2 C_2/4\pi)\beta$ which are the Debye length and the distance of closest approach. Thus

$$\frac{\eta_L}{\eta_0} \approx \frac{5\sqrt{3\pi}}{27}\frac{1}{\Gamma^{5/2}}\frac{1}{\ln(1/\Gamma)} \tag{8.15}$$

or $\eta_L/\eta_0 \approx 0.6/[\Gamma^{5/2}\ln(1/\Gamma)]$, which is overall consistent with our analysis.

The Landau or mean-field result is smaller for the viscosity than the result from perturbative QCD. Indeed, the unscaled Landau viscosity (8.15) reads

$$\frac{\eta_L}{\eta_0} \approx \frac{5}{12\sqrt{\pi}}\frac{\sqrt{m}}{(\alpha_s C_2)^2\beta^{5/2}}\frac{1}{\ln(1/\alpha_s)} \tag{8.16}$$

after restoring the viscosity unit $\eta_0 = nm\omega_p a_{WS}^2$ and using $\ln(r_D/r_0) \approx 3\ln(1/\alpha_s)/2$ with $\alpha_s = g^2/4\pi$. It is amusing to note that if we set $m \approx gT$ and $C_2 = N_c = 3$ in (8.16) we obtain

$$\eta_L \approx \frac{5\sqrt{2}}{108\pi^{1/4}}\frac{T^3}{\alpha_s^{7/4}\ln(1/\alpha_s)} \approx 0.05\frac{T^3}{\alpha_s^{7/4}\ln(1/\alpha_s)}, \tag{8.17}$$

which is to be compared with the QCD weak-coupling result [20,21]

$$\eta_{\rm QCD} \approx \frac{T^3}{\alpha_s^2\ln(1/\alpha_s)}. \tag{8.18}$$

IX. DIFFUSION CONSTANT

The calculation of the diffusion constant in the SU(2) plasma is similar to that of the shear viscosity. The governing equation is again (3.7) with Σ and $\mathbf{S}$ replaced by Σ_s, $\mathbf{S}_s$. The label is short for a single particle. The difference between $\mathbf{S}$ and $\mathbf{S}_s$ is the substitution of (2.7) by

$$f_s(\boldsymbol{r}\,\boldsymbol{p}\,\boldsymbol{Q}t) = \sqrt{N}\delta[\boldsymbol{r} - \boldsymbol{r}_1(t)]\delta[\boldsymbol{p} - \boldsymbol{p}_1(t)]\delta[\boldsymbol{Q} - \boldsymbol{Q}_1(t)]. \tag{9.1}$$

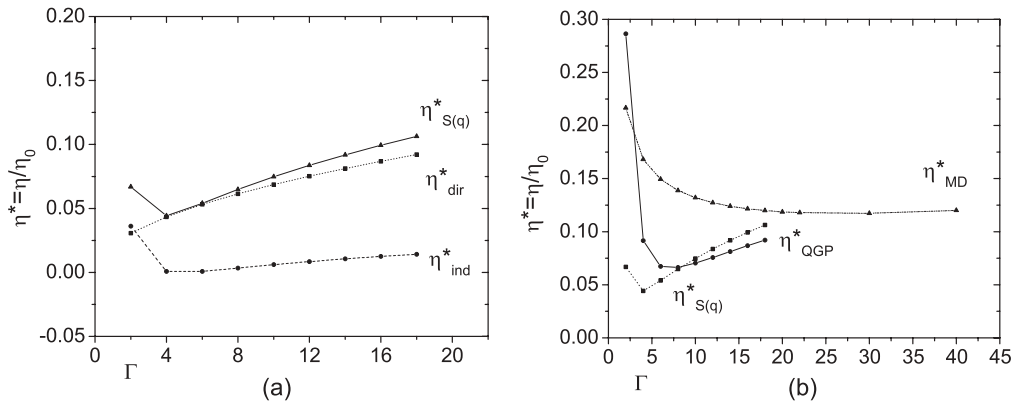

FIG. 5. Comparison with weak coupling. See the text.

The diffusion constant follows from the velocity autocorrelator

$$V_D(t) = \tfrac{1}{3}\langle \boldsymbol{V}(t)\cdot\boldsymbol{V}(0)\rangle \tag{9.2}$$

through

$$D = \int_0^\infty dt\, V_D(t). \tag{9.3}$$

Solving (3.7) using the method of one Sonine polynomial approximation as in [18] yields the Langevin-type equation

$$\frac{dV_D(t)}{dt} = -\int_0^t dt' M(t') V_D(t-t') \tag{9.4}$$

with the memory kernel tied to Σ^S_{C0},

$$\begin{aligned} & n\, f_0(\boldsymbol{p}')\, \Sigma^S_{Cl}(t,\boldsymbol{k},\boldsymbol{p}\boldsymbol{p}') \\ &= -\frac{1}{\beta}\int d\boldsymbol{p}_1 d\boldsymbol{p}_2 \int \frac{d\boldsymbol{l}}{(2\pi)^3}\boldsymbol{l}\cdot\nabla_p \boldsymbol{l}\cdot\nabla_{p'}\mathbf{c}_{D1}(l) V_l \\ &\quad\times\left(\frac{l}{2l+1}\mathbf{S}^S_{l-1}(t,\boldsymbol{k}-\boldsymbol{l},\boldsymbol{p}\boldsymbol{p}')\,\mathbf{S}_1(t,\boldsymbol{l},\boldsymbol{p}_1\boldsymbol{p}_2)\right. \\ &\quad\left.+\frac{l+1}{2l+1}\mathbf{S}^S_{l+1}(t,\boldsymbol{k}-\boldsymbol{l},\boldsymbol{p}\boldsymbol{p}')\,\mathbf{S}_1(t,\boldsymbol{l},\boldsymbol{p}_1\boldsymbol{p}_2)\right) \end{aligned} \tag{9.5}$$

and

$$\begin{aligned} & n\, f_0(\boldsymbol{p}')\, \Sigma^S_{C0}(t,\boldsymbol{k}=\mathbf{0},\boldsymbol{p}\boldsymbol{p}') \\ &= -\frac{1}{\beta}\int d\boldsymbol{p}_1 d\boldsymbol{p}_2 \int \frac{d\boldsymbol{l}}{(2\pi)^3}\boldsymbol{l}\cdot\nabla_p \boldsymbol{l}\cdot\nabla_{p'}\mathbf{c}_{D1}(l) \\ &\quad\times V_l \mathbf{S}^S_1(t,\boldsymbol{l},\boldsymbol{p}\boldsymbol{p}')\,\mathbf{S}_1(t,\boldsymbol{l},\boldsymbol{p}_1\boldsymbol{p}_2), \end{aligned} \tag{9.6}$$

therefore

$$M(t) = \frac{\beta}{3m}\int d\boldsymbol{p}\, d\boldsymbol{p}'\, p\cdot\boldsymbol{p}'\Sigma^S_{C0}(t,\boldsymbol{k}=\mathbf{0},\boldsymbol{p}\boldsymbol{p}')f_0(\boldsymbol{p}') \tag{9.7}$$

which clearly projects out the singlet color contribution. If we introduce the dimensionless diffusion constant, $D^* = D/w_p a^2_{\rm WS}$, then (9.3) together with (9.4) yield

$$\begin{aligned} \frac{1}{D} &= m\beta\int_0^\infty dt\, M(t) \to \frac{1}{D^*} \\ &= 3\Gamma\int_0^\infty w_p dt\frac{M(t)}{w_p^2} = 3\Gamma\int_0^\infty d\tau\,\bar{M}(\tau). \end{aligned} \tag{9.8}$$

Using similar steps as for the derivation of the viscosity, we can unwind the self-energy kernel Σ_s in (9.8) to give

$$\frac{1}{D^*} = -\Gamma\int\frac{d\boldsymbol{l}}{(2\pi)^3}\int_0^\infty d\tau\, l^2\mathbf{c}_{D1}(l)V_l\mathcal{G}^S_{n1}(l,t)\,\mathcal{G}_{n1}(l,t), \tag{9.9}$$

where we have used the same the half-renormalization method discussed above for the viscosity. The color integrations are done by Legendre transforms. Here again, we separate the time-dependent structure factors as $\mathcal{G}_{n1}(l,t) = \mathbf{S}_{01}(l)\bar{\mathcal{G}}_{n1}(l,t)$ and $\mathbf{S}^S_{01}(l,t) = \bar{\mathcal{G}}_{n1}(l,t)$ in the free-particle approximation. Thus

$$\frac{1}{D^*} = \Gamma^{3/2}\left(\frac{1}{3\pi}\right)^{\frac{1}{2}}\int_0^\infty dq\, q[1-\mathbf{S}_{01}(q)]. \tag{9.10}$$

TABLE II. Diffusion constant. See the text.

Γ	2	4	6	8	10	12	14	16	18
$D^*_{\rm QGP}$	0.410	0.115	0.055	0.034	0.024	0.017	0.014	0.012	0.010
$D^*_{\rm MD}$	0.230	0.132	0.095	0.076	0.063	0.055	0.048	0.044	0.040

The results following from (9.10) are displayed in Table II and in Fig. 6 (solid line) from weak to strong coupling. For comparison, we also show the diffusion constant measured using molecular-dynamics simulations with an SU(2) colored Coulomb plasma [3]. The molecular-dynamics simulations are fitted to

$$D^* \simeq \frac{0.4}{\Gamma^{0.8}}. \tag{9.11}$$

For comparison, we also show the diffusion constant (9.10) assessed using the weak coupling or Debye structure factor $S(k) = k^2/(k^2+k_D^2)$ in Fig. 6 (dotted line). The discrepancy between the analytical results at small Γ are similar to the ones we noted above for the shear viscosity. In our correctly resummed structure factor of Fig. 2, the infrared behavior of the cQGP is controlled in contrast to the simple Debye structure factor.

Finally, a comparison of (9.10) to (8.5) shows that $1/D^* \approx 1/\lambda I_3$ which is seen to grow like $\Gamma^{3/2}$. Thus D^* drops like $1/\Gamma^{3/2}$, which is close to the numerically generated result fitted in Fig. 7(a). The weak-coupling self-diffusion coefficient scales as $1/\Gamma^{5/2}$ as shown in Fig. 7(b). More importantly, the diffusion constant in the SU(2) colored Coulomb plasma is caused solely by the nonhydrodynamical modes or single-particle collisions in our analysis. It does not survive at strong coupling where most of the losses are caused by the collective sound and/or plasmon modes. This result is in contrast with the shear viscosity we discussed above, where the hydrodynamical modes level it off at large Γ.

The current analysis gives an analytical understanding to the numerical results of [3]. It is true that the nonrelativistic and classical description followed here yields particle number conservation, unlike the relativistic and quantum description. However, we think that our diffusion analysis sheds some

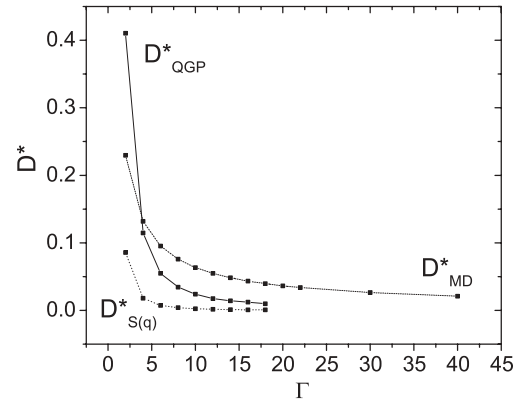

FIG. 6. Diffusion constant (solid and dotted lines) versus molecular-dynamics simulations (dashed line). See the text.

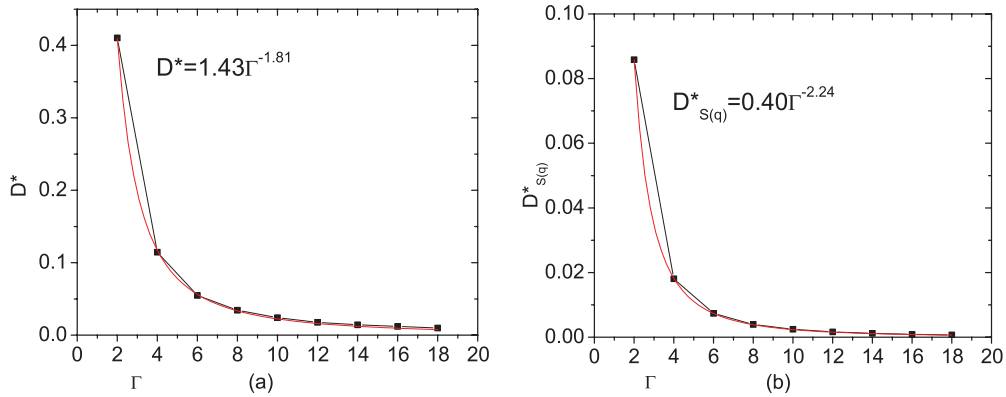

FIG. 7. (Color online) Fit to the diffusion constant. See the text.

light on the diffusion of conserved charges in QCD at strong coupling, e.g, fermion number, isospin number, etc.

X. CONCLUSIONS

We have provided a general framework for discussing nonperturbative many-body dynamics in the colored SU(2) Coulomb plasma introduced in [1]. The framework extends the analysis developed intially for one-component Abelian plasmas to the non-Abelian case. In the latter, the Liouville operator is supplemented by a color precessing contribution that contributes to the connected part of the self-energy kernel.

The many-body content of the SU(2) colored Coulomb plasma are best captured by the Liouville equation in phase space in the form of an eigenvaluelike equation. Standard projected perturbation theory, such as analysis around the static phase-space distributions yield a resummed self-energy kernel in closed form. Translational space invariance and rigid color rotational invariance in phase space simplifies the nature of the kernel.

In the hydrodynamical limit, the phase-space projected equations for the time-dependent and resummed structure factor displays both transverse and longitudinal hydrodynamical modes. The shear viscosity and longitudinal diffusion constant are expressed explicitly in terms of the resummed self-energy kernel. The latter is directly tied with the interacting part of the Liouville operator in color space. We have shown that in the free-streaming approximation and half-renormalized Liouville operators, the transport parameters are finite.

We have explicitly derived the shear viscosity and longitudinal diffusion constant of the SU(2) colored Coulomb plasma in terms of the monopole static structure factor and the for all values of the classical Coulomb parameter $\Gamma = V/K$, the ratio of the potential to kinetic energy per particle. The results compare fairly with molecular-dynamics simulations for SU(2).

The longitudinal diffusion constant is found to drop from weak to strong coupling like $1/\Gamma^{3/2}$. The shear viscosity is found to reach a minimum for Γ of about 8. The large increase at weak coupling is the result of the large mean free paths and is encoded in the direct or driving part of the connected self-energy. The minimum at intermediate Γ is tied to the onset of hydrodynamics which reflects on the liquid nature of the colored Coulomb plasma in this regime.

At larger values of Γ an SU(2) crystal forms as reported in [1]. Our current analysis should be able to account for the emergence of elasticities with, in particular, an elastic shear mode. This point will be pursued in a future investigation. The many-body analysis presented in this work treats the color degrees of freedom as massive constituents with a finite mass and a classical SU(2) color charge. The dynamical analysis is fully nonclassical. In a way, quantum mechanics is assumed to generate the constituent degrees of freedom with their assigned parameters. While this picture is supported by perturbation theory at very weak coupling, its justification at strong coupling is by no means established.

ACKNOWLEDGMENTS

This work was supported in part by US DOE Grants No. DE-FG02-88ER40388 and No. DE-FG03-97ER4014.

APPENDIX A: SU(2) COLOR PHASE SPACE

A useful parametrization of the SU(2) color phase space is through the canonical variables Q^1, π^1 [22,23]

$$Q^1 = \cos\phi_1\sqrt{J^2-\pi_1^2}, \qquad Q^2 = \sin\phi_1\sqrt{J^2-\pi_1^2}, \quad Q^3 = \pi^1 \tag{A1}$$

with Q^2 being a constraint variable fixed by J^2 or the quadratic Casimir with $q_2 = \sum_\alpha^{N_c^2-1} Q^\alpha Q^\alpha$. The conjugate set Q^1, π^1 obeys standard Poisson bracket. The associated phase-space measure is

$$dQ = c_R d\pi_1 d\phi_1 J dJ \delta(J^2 - q_2), \tag{A2}$$

where c_R is a representation-dependent constant. A simpler parametrization of the phase space is to use

$$dQ = \sin\theta d\theta d\phi \tag{A3}$$

with the normalizations $\int dQ = 4\pi$, $\sum_\alpha Q^\alpha Q^\alpha = 1$ and $\int dQ\, \boldsymbol{Q}\cdot\boldsymbol{Q} = 4\pi$. The SU(2) Casimir is then restored by inspection.

APPENDIX B: PROJECTION METHOD

If we define the phase-space density, $\delta f_l^m(\boldsymbol{kp},t)$,

$$\delta f_l^m(\boldsymbol{kp},t)=\sum_{i=1}^{N}e^{-ik\cdot r_i(t)}\delta[\boldsymbol{p}-\boldsymbol{p}_i(t)]Y_l^m(\boldsymbol{Q}_i)-nf_0(\boldsymbol{p})\delta_{l0}\delta_{m0}\delta_{k\mathbf{0}}Y_0^0, \tag{B1}$$

we can construct structure factor $\mathbf{S}_l(t,\boldsymbol{k},\boldsymbol{pp}')$ for the lth partial wave

$$\begin{aligned}&\frac{4\pi}{2l+1}\sum_m\left[\delta f_l^{m*}(\boldsymbol{kp},t)\middle|\delta f_l^m(\boldsymbol{kp}',0)\right]\\&\equiv\frac{4\pi}{2l+1}\sum_m\sum_{i,j}^{N}\left\{e^{-ik\cdot(r_i(t)-r_j(t))}\delta[\boldsymbol{p}-\boldsymbol{p}_i(t)]\delta(\boldsymbol{p}'-\boldsymbol{p}_j)\right.\\&\left.\times Y_l^{m*}(\boldsymbol{Q}_i)Y_l^m(\boldsymbol{Q}_j)\right\}-n^2f_0(\boldsymbol{p})f_0(\boldsymbol{p}')\\&\equiv\mathbf{S}_l(t,\boldsymbol{k},\boldsymbol{pp}').\end{aligned} \tag{B2}$$

Here a scalar product $(A|B)$ is defined as $\langle A^*B\rangle_{\rm eq}$. We follow [16,24,25] and recast the formal Liouville equation (3.4) in the form of a formal eigenvaluelike equation in phase space,

$$\mathbf{S}_l(\boldsymbol{k}z;\boldsymbol{pp}')=\left[\delta f_l^{m*}(\boldsymbol{kp})|(z-\mathcal{L})^{-1}|\delta f_l^m(\boldsymbol{k}'\boldsymbol{p}')\right]. \tag{B3}$$

The color charge effect by partial waves is represented as l,m in Eq. (B3). If we introduce the projection operator

$$\begin{aligned}\mathcal{P}=4\pi\sum_{l,m,k}\int d\boldsymbol{p}_1d\boldsymbol{p}_2\left|\delta f_l^m(\boldsymbol{k},\boldsymbol{p}_1)\right)\mathbf{S}_{0l}^{-1}(\boldsymbol{k},\boldsymbol{p}_1,\boldsymbol{p}_2)\\\times\left(\delta f_l^{m*}(\boldsymbol{k},\boldsymbol{p}_2)\right|=1-\mathcal{Q},\end{aligned} \tag{B4}$$

we can check that this projection operator satisfies $\mathcal{P}^2=\mathcal{P}$

$$\begin{aligned}\mathcal{P}^2=4\pi\sum_{l,m,\boldsymbol{k}}\sum_{l',m',\boldsymbol{k}'}\int d\boldsymbol{p}_1d\boldsymbol{p}_2d\boldsymbol{p}_1'd\boldsymbol{p}_2'\left|\delta f_l^m(\boldsymbol{k},\boldsymbol{p}_1)\right)\\\times\mathbf{S}_{0l}^{-1}(\boldsymbol{k},\boldsymbol{p}_1,\boldsymbol{p}_2)4\pi\left(\delta f_l^{m*}(\boldsymbol{k},\boldsymbol{p}_2)\right|\delta f_{l'}^{m'}(\boldsymbol{k},\boldsymbol{p}_1')\right)\\\times\mathbf{S}_{0l}^{-1}(\boldsymbol{k},\boldsymbol{p}_1{}',\boldsymbol{p}_2{}')\left(\delta f_{l'}^{m'*}(\boldsymbol{k},\boldsymbol{p}_2{}')\right|=\mathcal{P}\end{aligned} \tag{B5}$$

because of the translational invariance in space and the rotational invariance in color space,

$$4\pi\left(\delta f_l^{m*}(\boldsymbol{k},\boldsymbol{p}_2)\middle|\delta f_{l'}^{m'}(\boldsymbol{k},\boldsymbol{p}_1')\right)\equiv\delta_{k2k'}\delta_{ll'}\delta_{mm'}\mathbf{S}_{0l}(\boldsymbol{k},\boldsymbol{p}_2,\boldsymbol{p}_1{}'). \tag{B6}$$

The off-diagonal elements vanish in the equilibrium averaging due to phase incoherence. Therefore, the projection operator in Eq. (B5) satisfies also $\mathcal{Q}^2=\mathcal{Q}$ and $\mathcal{PQ}=\mathcal{QP}=0$. If we define $|F_l^m(\boldsymbol{kp};z))$ as $|F_l^m(\boldsymbol{kp};z))=(z-\mathcal{L})^{-1}|\delta f_l^m(\boldsymbol{kp}))$ from Eq. (B3), we have

$$\mathcal{P}(z-\mathcal{L})\left|F_l^m(\boldsymbol{kp};z)\right)=\mathcal{P}\left|\delta f_l^m(\boldsymbol{kp})\right). \tag{B7}$$

$\mathcal{P}$ in Eq. (B5) is the operator which projects phase-space function of a multiparticle state with lth partial wave into a single-particle state of the same partial wave, $|\delta f_{l'}^{m'}(\boldsymbol{kp}))$, $\mathcal{P}|g_{l'}^{m'}(\boldsymbol{kp}))=|\delta f_{l'}^{m'}(\boldsymbol{kp}))$. Therefore $\mathcal{Q}|\delta f_l^m(\boldsymbol{kp}))=(1-\mathcal{P})|\delta f_l^m(\boldsymbol{kp}))=0$. With these in mind, we can modify the above equation further using $\mathcal{P}+\mathcal{Q}=I$,

$$\begin{aligned}(\mathcal{P}z-\mathcal{PLP}-\mathcal{PLQ})\left|F_l^m(\boldsymbol{kp};z)\right)&=\mathcal{P}\left|\delta f_l^m(\boldsymbol{kp})\right),\\(\mathcal{Q}z-\mathcal{QLP}-\mathcal{QLQ})\left|F_l^m(\boldsymbol{kp};z)\right)&=0.\end{aligned} \tag{B8}$$

From these equations, we can extract

$$\begin{aligned}&z\mathcal{P}\left|F_l^m(\boldsymbol{kp};z)\right)-\mathcal{PLP}\left|F_l^m(\boldsymbol{kp};z)\right)-\mathcal{PLQ}(z-\mathcal{QLQ})^{-1}\\&\times\mathcal{QLP}\left|F_l^m(\boldsymbol{kp};z)\right)=\mathcal{P}\left|\delta f_l^m(\boldsymbol{kp})\right).\end{aligned} \tag{B9}$$

By multiplying $(\delta f(\boldsymbol{kp})|$ we finally obtain

$$\begin{aligned}&z\mathbf{S}_l(\boldsymbol{k}z;\boldsymbol{pp}')-\int d\boldsymbol{p}_1d\Sigma_l(\boldsymbol{k}z;\boldsymbol{pp}_1)\mathbf{S}_l(\boldsymbol{k}z;\boldsymbol{p}_1\boldsymbol{p}')\\&=\mathbf{S}_l(\boldsymbol{k}0;\boldsymbol{pp}'),\end{aligned} \tag{B10}$$

where the memory function, or the evolution operator $\Sigma_l(\boldsymbol{k}z;\boldsymbol{pp}_1)$, is

$$\begin{aligned}\Sigma_l(\boldsymbol{k}z;\boldsymbol{pp}')=\frac{4\pi}{2l+1}\sum_m\int d\boldsymbol{p}_1\left(\delta f_l^{m*}(\boldsymbol{k},\boldsymbol{p})\right|\mathcal{L}\\+\Psi\left|\delta f_l^m(\boldsymbol{k},\boldsymbol{p}_1)\right)\mathbf{S}_{0l}^{-1}(\boldsymbol{k},\boldsymbol{p}_1,\boldsymbol{p}')\end{aligned} \tag{B11}$$

with

$$\Psi=\mathcal{PLQ}(z-\mathcal{QLQ})^{-1}\mathcal{QLP}. \tag{B12}$$

Since the Liouville operator $\mathcal{L}$ can be split into $\mathcal{L}_0+\mathcal{L}_I+\mathcal{L}_Q$, Eq. (2.9), the evolution operator can also be split into four terms; the free-streaming term (Σ_l^0), the self-consistent term (Σ_l^s), the color charge term (Σ^Q), and the nonlocal collision term (Σ^c),

$$\begin{aligned}\Sigma_{0l}(\boldsymbol{k}z;\boldsymbol{pp}')&=\frac{\boldsymbol{k}\cdot\boldsymbol{p}}{m}\delta(\boldsymbol{p}-\boldsymbol{p}'),\\\Sigma_{Il}(\boldsymbol{k}z;\boldsymbol{pp}')&=-n\frac{\boldsymbol{k}\cdot\boldsymbol{p}}{m}f_0(\boldsymbol{p})\mathbf{c}_{Dl}(\boldsymbol{k}),\\\Sigma_{Ql}(\boldsymbol{k}z;\boldsymbol{pp}')&=0,\\\Sigma_{Cl}(\boldsymbol{k}z;\boldsymbol{pp}')&=\frac{1}{nf_0(\boldsymbol{p})}\frac{4\pi}{2l+1}\sum_m\left(\delta f_l^{m*}(\boldsymbol{kp})\right|\\&\quad\times\mathcal{LQ}(z-\mathcal{QLQ})^{-1}\mathcal{QL}\left|\delta f_l^m(\boldsymbol{kp}')\right).\end{aligned} \tag{B13}$$

APPENDIX C: COLLISIONAL COLOR CONTRIBUTION

In this appendix we detail the calculation that leads to a zero contribution from the colored Liouville operator in the collisional part of the self-energy in the free-streaming approximation. A typical contribution to (5.2) and (5.5) is

$$\begin{aligned}&L_Q(\boldsymbol{q},\boldsymbol{q}_1)\,L_Q^R(\boldsymbol{q}',\boldsymbol{q}_2)\,\mathbf{S}(t,\boldsymbol{q},\boldsymbol{q}_2)\,\mathbf{S}(t,\boldsymbol{q}',\boldsymbol{q}_1)\\&=\frac{1}{\beta}\left[V(\boldsymbol{r}-\boldsymbol{r}_1)\,\boldsymbol{Q}\times\boldsymbol{Q}_1\cdot(\nabla_Q-\nabla_{Q_1})\right]\\&\quad\times\left[\mathbf{c}_D'(\boldsymbol{r}'-\boldsymbol{r}_2,\,\boldsymbol{Q}'\cdot\boldsymbol{Q}_2)\,\boldsymbol{Q}'\times\boldsymbol{Q}_2\cdot(\nabla_{Q'}-\nabla_{Q_2})\right]\\&\quad\times\mathbf{S}(t,\boldsymbol{q},\boldsymbol{q}_2)\,\mathbf{S}(t,\boldsymbol{q}',\boldsymbol{q}_1).\end{aligned} \tag{C1}$$

which can be reduced to

$$\begin{aligned}&L_Q(\boldsymbol{q},\boldsymbol{q}_1)\,L_Q^R(\boldsymbol{q}',\boldsymbol{q}_2)\,\mathbf{S}(t,\boldsymbol{q},\boldsymbol{q}_2)\,\mathbf{S}(t,\boldsymbol{q}',\boldsymbol{q}_1)\\&=-\frac{1}{\beta}V(\boldsymbol{r}-\boldsymbol{r}_1)\,\mathbf{c}_D'(\boldsymbol{r}'-\boldsymbol{r}_2,\,\boldsymbol{Q}'\cdot\boldsymbol{Q}_2)\\&\quad\times[\mathbf{S}'(\boldsymbol{Q}\cdot\boldsymbol{Q}_2)\mathbf{S}'(\boldsymbol{Q}'\cdot\boldsymbol{Q}_1)(\boldsymbol{Q}_1\times\boldsymbol{Q}_2)\cdot\boldsymbol{Q}\,(\boldsymbol{Q}_1\times\boldsymbol{Q}_2)\cdot\boldsymbol{Q}'\end{aligned}$$

$$\times \mathbf{S}''(\boldsymbol{Q}\cdot\boldsymbol{Q}_2)\mathbf{S}(\boldsymbol{Q}'\cdot\boldsymbol{Q}_1)(\boldsymbol{Q}_1\times\boldsymbol{Q}_2)\cdot\boldsymbol{Q}(\boldsymbol{Q}\times\boldsymbol{Q}')\cdot\boldsymbol{Q}_2$$
$$\times \mathbf{S}(\boldsymbol{Q}\cdot\boldsymbol{Q}_2)\mathbf{S}''(\boldsymbol{Q}'\cdot\boldsymbol{Q}_1)(\boldsymbol{Q}\times\boldsymbol{Q}')\cdot\boldsymbol{Q}_1(\boldsymbol{Q}_1\times\boldsymbol{Q}_2)\cdot\boldsymbol{Q}'$$
$$\times \mathbf{S}'(\boldsymbol{Q}\cdot\boldsymbol{Q}_2)\mathbf{S}'(\boldsymbol{Q}'\cdot\boldsymbol{Q}_1)(\boldsymbol{Q}\times\boldsymbol{Q}')\cdot\boldsymbol{Q}_1(\boldsymbol{Q}\times\boldsymbol{Q}')\cdot\boldsymbol{Q}_2]. \quad \text{(C2)}$$

The derivatives on $\mathbf{c}_D$ and $\mathbf{S}$ are on their color argument. We note that (C2) contributes to the collisional part of the self-energy in (B6) after the integration over Q_1 and Q_2, which is then zero. This is expected. Indeed, the colored Liouville operator is a three-body force that requires three distinct color charges to not vanish. While (C2) contributes to the unintegrated collisional operator, it does not in the integrated one, which is the self-energy on the two-point function. It does contribute in the Liouville hierarchy in the three-body structure factors and higher.

APPENDIX D: HYDRODYNAMICAL SUBSPACE

The projection method onto the hydrodynamical subspace has been discussed by many [11,12,16]. This consists in dialing the projector in (6.2) onto the hydrodynamical modes. We choose Hermite polynomials as a basis set with the Maxwell-Boltzmann distribution $f_0(\boldsymbol{p})$ as a Gaussian weight function. The Hermite polynomials are the generalized ones in three dimensions [26]. Specifically,

$$H_{1(n)}(\boldsymbol{p})=1,\quad H_{2(l)}(\boldsymbol{p})=p_z,\quad H_{3(\epsilon)}(\boldsymbol{p})=\frac{1}{\sqrt{6}}(p^2-3),$$
$$H_{4(t_1)}(\boldsymbol{p})=p_x,\quad H_{5(t_2)}(\boldsymbol{p})=p_y. \quad \text{(D1)}$$

These polynomials are orthonormal for the inner product

$$\langle m|n\rangle = \int d\boldsymbol{p}\, a_m H_m(\boldsymbol{p}) a_n H_n(\boldsymbol{p}) n f_0(\boldsymbol{p}) = \delta_{mn},$$
$$\langle m|F(k,t)|n\rangle = \int d\boldsymbol{p}\, d\boldsymbol{p}'\, a_m H_m(\boldsymbol{p}) F(k,t;\boldsymbol{p}\boldsymbol{p}') a_n \times H_n(\boldsymbol{p}') n f_0(\boldsymbol{p}'). \quad \text{(D2)}$$

Here a_m and a_n set the normalizations. We chose the longitudinal momentum direction along $\boldsymbol{k}$ in Fourier space, $\langle l| = a_m \hat{k}\cdot\boldsymbol{p}$. The transverse directional is chosen orthogonal to $\boldsymbol{k}$, $\langle t| = a'_m \boldsymbol{\epsilon}\cdot\boldsymbol{p}$ with a unit vector satisfying $\boldsymbol{\epsilon}^2=1$ and $\boldsymbol{\epsilon}\cdot\hat{k}=0$.

The hydrodynamical projection operators $\mathcal{P}_H$ restricted to the five states (D1) are

$$\mathcal{P}_H=\sum_i^5 |i\rangle\langle i|,\quad \mathcal{Q}_H=1-\mathcal{P}_H=1-\sum_i^5 |i\rangle\langle i|. \quad \text{(D3)}$$

While in general these five states are enough to characterize the hydrodynamical modes in the SU(2) phase space, we need additional states to work out the shear viscosity as it involves in general correlations in the stress tensor through the Kubo relation [27]. For that we need additionally

$$H_6(\boldsymbol{p})=p_x p_y,\quad H_7(\boldsymbol{p})=p_x p_z,\quad H_8(\boldsymbol{p})=p_y p_z. \quad \text{(D4)}$$

With the definition of $G_{ij}(\boldsymbol{k}z)=\langle i|\mathbf{S}(\boldsymbol{k}z;\boldsymbol{p}\boldsymbol{p}')[nf_0(\boldsymbol{p})]^{-1}|j\rangle$ we can rewrite (6.2) as

$$\left(z-\sum\langle i|\Omega(\boldsymbol{k}z;\boldsymbol{p}\boldsymbol{p}')|k\rangle\right)G_{kj}(\boldsymbol{k}z)=G_{ij}(\boldsymbol{k}0), \quad \text{(D5)}$$

where i, $j^k$are short for n (density), ϵ (energy), l (longitudinal momentum), and t (transverse momentum).

[1] E. V. Shuryak and I. Zahed, Phys. Rev. C **70**, 021901 (2004); Phys. Rev. D **70**, 054507 (2004).
[2] D. Teaney, J. Lauret, and E. V. Shuryak, Phys. Rev. Lett. **86**, 4783 (2001); arXiv:nucl-th/0110037; P. F. Kolb, P. Huovinen, U. Heinz, and H. Heiselberg, Phys. Lett. B **500**, 232 (2001); P. F. Kolb and U. Heinz, in *Quark-Gluon Plasma 3*, edited by R. C. Hwa and X. N. Wang (World Scientific, Singapore, 2004), p. 634, nucl-th/0305084.
[3] B. A. Gelman, E. V. Shuryak, and I. Zahed, Phys. Rev. C **74**, 044908 (2006).
[4] S. Cho and I. Zahed, Phys. Rev. C **79**, 044911 (2009).
[5] S. Cho and I. Zahed, Phys. Rev. C **80**, 014906 (2009).
[6] K. Dusling and I. Zahed, Nucl. Phys. A **833**, 172 (2010).
[7] P. Petreczky, F. Karsch, E. Laermann, S. Stickan, and I. Wetzorke, Nucl. Phys. Rev. Proc. Suppl. **106–107**, 513 (2002).
[8] B. A. Gelman, E. V. Shuryak, and I. Zahed, Phys. Rev. C **74**, 044909 (2006).
[9] S. K. Wong, Nuovo Cimento A **65**, 689 (1970).
[10] S. Cho and I. Zahed, Phys. Rev. C **82**, 044905 (2010).
[11] D. Foster and P. C. Martin, Phys. Rev. A **2**, 1575 (1970).
[12] D. Foster, Phys. Rev. A **9**, 943 (1974).
[13] G. F. Mazenko, Phys. Rev. A **7**, 209 (1973).
[14] G. F. Mazenko, Phys. Rev. A **9**, 360 (1974).
[15] J. Wallenborn and M. Baus, Phys. Rev. A **18**, 1737 (1978).
[16] M. Baus, Physica A **79**, 377 (1975).
[17] S. Cho and I. Zahed, arXiv:0910.1548.
[18] H. Gould and G. F. Mazenko, Phys. Rev. A **15**, 1274 (1977).
[19] S. Ichimaru, *Statistical Plasma Physics, Vol I: Basic Principles* (Westview Press, Boulder, CO, 2004).
[20] A. Hosoya and K. Kajantie, Nucl. Phys. B **250**, 666 (1985).
[21] G. Baym, H. Monien, C. J. Pethick, and D. G. Ravenhall, Phys. Rev. Lett. **64**, 1867 (1990).
[22] K. Johnson, Ann. Phys. **192**, 104 (1989).
[23] D. F. Litim and C. Manuel, Phys. Rep. **364**, 451 (2002).
[24] H. Mori, Prog. Theor. Phys. **33**, 423 (1965).
[25] A. Z. Akcasu and J. J. Duderstadt, Phys. Rev. **188**, 479 (1969).
[26] H. Grad, Commun. Pure Appl. Math. **2**, 331 (1949).
[27] J. P. Hansen and I. R. McDonald, *Theory Of Simple Liquids*, 3rd eds. (Academic Press, New York, 2006).